BASIC AND TRANSLATIONAL—LIVER

Monoacylglycerol Lipase Controls Endocannabinoid and Eicosanoid Signaling and Hepatic Injury in Mice

ZONGXIAN CAO,[1] MELINDA M. MULVIHILL,[2] PARTHA MUKHOPADHYAY,[1] HUAN XU,[1] KATALIN ERDÉLYI,[1] ENKUI HAO,[1,3] EILEEN HOLOVAC,[1] GYÖRGY HASKÓ,[4] BENJAMIN F. CRAVATT,[5] DANIEL K. NOMURA,[2,§] and PÁL PACHER[1,§]

[1]Section on Oxidative Stress and Tissue Injury, Laboratory of Physiological Studies, National Institutes of Health/National Institute on Alcohol Abuse and Alcoholism, Bethesda, Maryland; [2]Program in Metabolic Biology, Department of Nutritional Sciences and Toxicology, University of California Berkeley, Berkeley, California; [3]Department of Cardiology, Jinan Central Hospital (affiliated with Shandong University), Jinan, Shandong, China; [4]Department of Surgery, University of Medicine and Dentistry of New Jersey–New Jersey Medical School, Newark, New Jersey; and [5]Department of Chemical Physiology, The Scripps Research Institute, Skaggs Institute for Chemical Biology, La Jolla, California

BACKGROUND & AIMS: The endocannabinoid and eicosanoid lipid signaling pathways have important roles in inflammatory syndromes. Monoacylglycerol lipase (MAGL) links these pathways, hydrolyzing the endocannabinoid 2-arachidonoylglycerol to generate the arachidonic acid precursor pool for prostaglandin production. We investigated whether blocking MAGL protects against inflammation and damage from hepatic ischemia/reperfusion (I/R) and other insults. **METHODS:** We analyzed the effects of hepatic I/R in mice given the selective MAGL inhibitor JZL184, in *Mgll*$^{-/-}$ mice, *fatty acid amide hydrolase*$^{-/-}$ mice, and in *cannabinoid receptor type 1*$^{-/-}$ (CB_1-/-) and *cannabinoid receptor type 2*$^{-/-}$ (CB_2-/-). Liver tissues were collected and analyzed, along with cultured hepatocytes and Kupffer cells. We measured endocannabinoids, eicosanoids, and markers of inflammation, oxidative stress, and cell death using molecular biology, biochemistry, and mass spectrometry analyses. **RESULTS:** Wild-type mice given JZL184 and *Mgll*$^{-/-}$ mice were protected from hepatic I/R injury by a mechanism that involved increased endocannabinoid signaling via CB_2 and reduced production of eicosanoids in the liver. JZL184 suppressed the inflammation and oxidative stress that mediate hepatic I/R injury. Hepatocytes were the major source of hepatic MAGL activity and endocannabinoid and eicosanoid production. JZL184 also protected from induction of liver injury by D-(+)-galactosamine and lipopolysaccharides or CCl_4. **CONCLUSIONS: MAGL modulates hepatic injury via endocannabinoid and eicosanoid signaling; blockade of this pathway protects mice from liver injury. MAGL inhibitors might be developed to treat conditions that expose the liver to oxidative stress and inflammatory damage.**

Keywords: Mouse Model; Endocannabinoid Signaling; Eicosanoid Production; Surgery.

Hepatic ischemia/reperfusion (I/R) injury is a major cause of morbidity and mortality in patients undergoing liver surgery/resection and transplantation.[1,2] Inflammation and generation of reactive oxygen and nitrogen stress in the liver underlie the hepatic cell death, dysfunction, and ultimate organ failure arising from hepatic I/R. Anti-inflammatory agents thus have been proposed as one treatment strategy for improving the clinical outcome of surgical procedures involving liver resections or transplant.[2] Anti-inflammatory drugs that block cyclooxygenases (COX1 and COX2) and reduce proinflammatory eicosanoids, as well as cannabinoid agonists that stimulate the anti-inflammatory cannabinoid receptor type 2 (CB_2 or *Cnr2*), exert significant hepatoprotective effects in liver of rodents exposed to I/R.[3–5] Both COX1- and COX2-selective and dual COX1/COX2 inhibition or genetic ablation of COX2 have been shown to confer protection against hepatic damage caused by I/R by attenuating neutrophil recruitment and cell death in the liver.[4,6] Studies also have shown that vasoconstrictive eicosanoids such as thromboxane A2 induce hepatic damage through platelet aggregation, induction of leukocyte adhesion, and increases in proinflammatory cytokines.[7] Previous studies have shown that hepatic I/R leads to significant increases in endogenous ligands for the cannabinoid receptors (endocannabinoids) 2-arachidonoylglycerol (2-AG) and anandamide.[1] Anandamide is considered to be a partial or full agonist of CB_1 receptors, depending on the tissue and biological response measured, and it has very low efficacy at CB_2 receptors. In contrast, 2-AG is considered to be the natural ligand for CB_2 receptors.[8] Consistent with an important role of endocannabinoids and CB_2 signaling in protecting liver

§Authors share co-senior authorship.

Abbreviations used in this paper: AA, arachidonic acid; 2-AG, arachidonoylglycerol; ALT, alanine aminotransferase; AST, aspartate aminotransferase; CB2R/*Cnr2*, cannabinoid receptor type 2; COX, cyclooxygenases; GalN, D-(+)-galactosamine; IP, intraperitoneal; I/R, ischemia/reperfusion; KC, Kupffer cells; LPS, lipopolysaccharide; MAGL/*Mgll*, monoacylglycerol lipase; mRNA, messenger RNA; NPC, nonparenchymal cells; TNF, tumor necrosis factor.

0016-5085/$36.00
http://dx.doi.org/10.1053/j.gastro.2012.12.028

against ischemic injury, *Cnr2*$^{-/-}$ mice develop increased I/R-induced inflammation and liver damage, and CB_2 agonists suppress hepatic proinflammatory cytokine and chemokine production, inflammatory cell infiltration, and oxidative and nitrative stress.[8] In contrast, inhibition of CB_1 is protective, suggesting an opposing regulatory role of this signaling in mediating liver injury.[9–13] Similar opposing regulatory roles of $CB_{1/2}$ signaling recently were described in models of atherosclerosis, kidney and brain injury, and hepatic fibrosis.[8]

We recently discovered that the endocannabinoid and eicosanoid systems are metabolically coupled through the action of monoacylglycerol lipase (MAGL or *Mgll*), which hydrolyzes 2-AG to produce the arachidonic acid (AA) precursor pools for eicosanoid biosynthesis.[14] Blocking MAGL reduces eicosanoids and neuroinflammatory responses in the brain and protects against neurodegeneration.[14] It remains unknown whether MAGL also plays a protective role in peripheral organs and, if so, by what mechanism. Here, we hypothesized that MAGL blockade might provide protection against inflammation and damage inflicted by hepatic I/R through either enhancing endocannabinoid signaling or suppressing eicosanoid production, or a combination of both pathways.

Materials and Methods

Mice and Chemicals

Six- to 8-week-old C57BL/6 mice were purchased from Jackson Laboratory (Bar Harbor, ME). *Mgll*$^{-/-}$ mice were generated previously.[15] JZL184 was purchased from Tocris Bioscience (Bristol, United Kingdom). CB_1 (SR141716A [SR1]/rimonabant) and CB_2 antagonists (SR144528 [SR2]) were obtained from NIDA Drug Supply Program (Research Triangle Park, NC). All these pharmacologic reagents were dissolved in 18:1:1 saline: Tween 80:dimethyl sulfoxide and administered by intraperitoneal (IP) injection at 10 μL/g mouse body weight.

Induction of Hepatic I/R

Partial hepatic I/R (1 h of ischemia followed by reperfusion for 2, 6, or 24 h) was induced as previously described[3,5,16,17] and is described in further detail in the Supplementary Materials and Methods section. JZL184, $CB_{1/2}$ antagonists were administered by IP injection at various time points (1 h before ischemia, and 1 and 3 h after reperfusion) as indicated. This animal study was approved by the Institutional Animal Care and Use Committees of the National Institute on Alcohol Abuse and Alcoholism, and has been performed in line with the National Institutes of Health guidelines for the care and use of laboratory animals.

Measurement of Endocannabinoids and Eicosanoids

Endocannabinoids and eicosanoids were measured using single-reaction monitoring–based liquid chromatography–tandem mass spectrometry analysis, as previously described[14] and detailed in the Supplementary Materials and Methods section.

Determination of Liver Damage and Injury

The activities of aspartate aminotransferase (AST) and alanine aminotransferase (ALT) were measured in serum samples using a clinical chemistry analyzer system (VetTest 8008; IDEXX Laboratories, Westbrook, ME). Histologic analysis of liver tissue damage was assessed by standard H&E staining of the tissue sections (5-μm thickness). For immunohistochemical staining of hepatic neutrophils, a primary antibody against mouse myeloperoxidase (Biocare Medical, Concord, CA) was used.

Determination of Inflammation, Oxidative Stress, and Cell Death

Inflammatory, oxidative stress, and cell death markers were quantified based on previously established procedures.[3,16] Please see the Supplementary Materials and Methods section for more details.

Isolation of Hepatocytes, Nonparenchymal Cells, and Kupffer Cells From Mouse Liver

Cell isolation from mouse liver was performed as described previously[18,19] and is detailed in the Supplementary Materials and Methods section. Briefly, mouse liver was perfused in situ with a solution containing 0.075% type IV collagenase (Sigma, St. Louis, MO). After mechanical dissociation and further digestion in 0.009% collagenase, hepatocytes and nonparenchymal cells (NPCs) were isolated by a series of gradient centrifugation using Percoll (GE Healthcare Bio-Sciences, Uppsala, Sweden). Kupffer cells (KCs) were purified using the MACS system (Miltenyi Biotec, Auburn, CA) after immunostaining with a monoclonal anti-F4/80 antibody and subsequent magnetic labeling.

Hypoxia-Reoxygenation Treatment of Isolated Mouse Hepatocytes

The cultured mouse hepatocytes were treated with 2-AG or JZL184 for 4 hours, and then were subjected to hypoxia (1% O_2) for 12 hours followed by reoxygenation for an additional 12 hours. Hepatocellular death induced by hypoxia-reoxygenation was estimated by measuring lactate dehydrogenase and ALT levels of the culture medium as described in the Supplementary Materials and Methods section.

Mouse KC Cultures and Treatments

Purified KCs were seeded into 96-well plates in RPMI supplemented with 10% bovine serum albumin, and were allowed to adhere to the plates for 12 hours. The cells were pretreated with AM630 and then were incubated with various concentrations of 2-AG for 4 hours at 37°C, followed by stimulation with lipopolysaccharide (LPS). After 90 minutes, culture media were collected and assayed for tumor necrosis factor α (TNFα) using an enzyme-linked immunosorbent assay kit (R&D, Minneapolis, MN).

Murine Hepatitis Models Induced by D-(+)-Galactosamine/LPS or CCl_4

C57BL/6 mice were treated IP with 800 mg/kg of D-(+)-galactosamine (GalN; Sigma) together with 1 μg/kg of LPS (from *Escherichia coli* 0127:B8; Sigma). The mice were euthanized 7–8 hours after GalN/LPS challenge, and blood and liver tissues were collected. For lethality study, LPS was used at a dose of 1.5 μg/kg, and mortality was assessed up to 8 hours after GalN/LPS challenge. JZL184-treated mice received an injection of 20 mg/kg of JZL184 IP 30 minutes before GalN/LPS treatment. For CCl_4-induced liver injury, mice were injected IP with 2 mL/kg of 10%

CCl_4 (Sigma) diluted in olive oil. The mice were killed 24 hours after CCl_4 injection, and the blood and livers were collected to assess liver injury.

Statistical Analysis

The results were expressed as the mean ± standard error of the mean. Differences among experimental groups were evaluated by the Student *t* test or analysis of variance whenever appropriate, and the significance of differences between groups was assessed by the Newman–Keuls post hoc test. The analysis was performed using a statistical software package (GraphPad Prism 5; GraphPad, La Jolla, CA). Significance was defined as a *P* value less than .05.

Results

Hepatic I/R Results in Dysregulated Endocannabinoid and Eicosanoid Metabolism

Consistent with our previous studies,[1] liver 2-AG and anandamide levels were increased substantially 6 hours after I/R in mice, concomitant with higher levels of both AA and eicosanoids prostaglandin E2, prostaglandin D2, and thromboxane B2 (Figure 1*A*). We found that pharmacologic (selective MAGL inhibitor JZL184, 40 mg/kg, IP) or genetic (*Mgll*$^{-/-}$ mice) inactivation of MAGL further enhanced 2-AG levels and decreased the levels of AA and eicosanoids below basal levels in the liver 2 and 6 hours after I/R, respectively (Figure 1*A* and *B*, Supplementary Figure 1). Inactivation of MAGL had no effect on early I/R-induced (I/R 2 h) increased COX-2 messenger RNA (mRNA) expression, despite reductions in eicosanoids, suggesting that during early I/R MAGL blockade decreases eicosanoids, likely by directly controlling the AA pool that generates eicosanoids in the liver (Supplementary Figure 2). However, hepatic COX-2 mRNA and protein expression were attenuated by MAGL blockade at 24 hours of reperfusion (I/R 24 h) (Supplementary Figure 2), suggesting that during later I/R MAGL blockade suppresses COX-2 expression, which also might contribute to the reduced eicosanoids in the liver. The reductions in AA and eicosanoids were not blocked by treatment with CB_1 or CB_2 antagonists (Supplementary Figure 1), excluding cannabinoid-mediated mechanisms for suppressing eicosanoid synthesis. Although JZL184 increased basal anandamide levels in mice with sham surgery, likely owing to a partial blockade of the anandamide hydrolyzing enzyme, fatty acid amide hydrolase,[20] neither pharmacologic nor genetic ablation of MAGL altered anandamide levels in the liver 6 hours after I/R (Figure 1*A* and *B*). These data thus indicate that the heightened levels of eicosanoids observed in hepatic I/R largely are derived from AA released by MAGL hydrolysis of 2-AG.

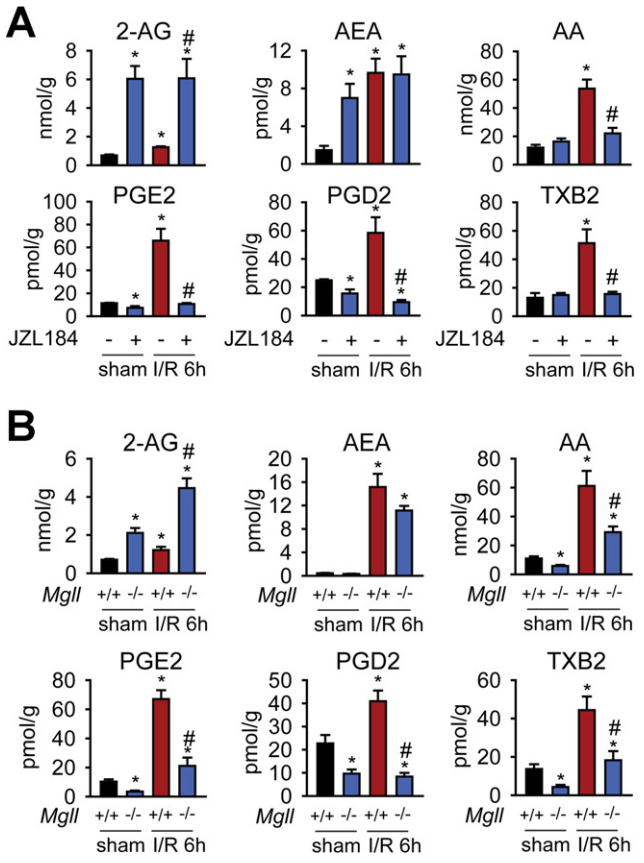

Figure 1. MAGL inactivation exerts bidirectional control over endocannabinoid and eicosanoid levels during hepatic I/R. (*A*) Pharmacologic and (*B*) genetic inactivation of MAGL enhances 2-AG levels but does not affect the levels of the other endocannabinoid anandamide in the liver. (*A* and *B*) MAGL blockade also lowers AA and eicosanoids in the I/R livers, measured after 6 hours of reperfusion (peak injury). The potent and selective MAGL inhibitor JZL184 (40 mg/kg, IP) was given 1 hour before inducing ischemia in the liver and endocannabinoid and eicosanoid levels were measured after 6 hours of reperfusion after ischemia by single-reaction monitoring–based liquid chromatography–tandem mass spectrometry analysis. Data represent mean ± standard error of the mean of 4–5 mice/group. Significance is represented as $^{*}P < .05$ between all groups vs sham vehicle-treated groups or sham *Mgll*$^{+/+}$ groups, and $^{\#}P < .05$ between JZL184-treated or *Mgll*$^{-/-}$ I/R groups and the I/R vehicle-treated or *Mgll*$^{+/+}$ groups. AEA, anandamide; PG, prostaglandin; TXB2, thromboxane B2.

MAGL Inactivation Attenuates Hepatic I/R-Induced Tissue Injury

We next asked whether blocking MAGL protects the liver against hepatic I/R-induced cell death and damage. Both genetic and preventative pharmacologic blockade (1 h before ischemia) of MAGL provided substantial hepatoprotection against I/R-induced liver injury, evidenced by attenuated serum levels of the acute liver damage/necrosis markers ALT and AST (Figure 2*A*, Supplementary Figure 3*A*), decreased coagulation necrosis seen in histologic sections (Figure 2*B*, Supplementary Figure 3*B*), as well as a decrease in delayed markers of apoptotic/necrotic cell demise (Figure 2*C*, Supplementary Figure 4). These protective effects were not observed during genetic or pharmacologic inactivation of fatty acid amide hydrolase (Supplementary Figure 5).

MAGL Inactivation Attenuates Hepatic I/R-Induced Inflammation and Oxidative Stress

We next sought to investigate the pathophysiologic mechanisms behind the hepatoprotective effect of MAGL inactivation on I/R-induced liver injury. We

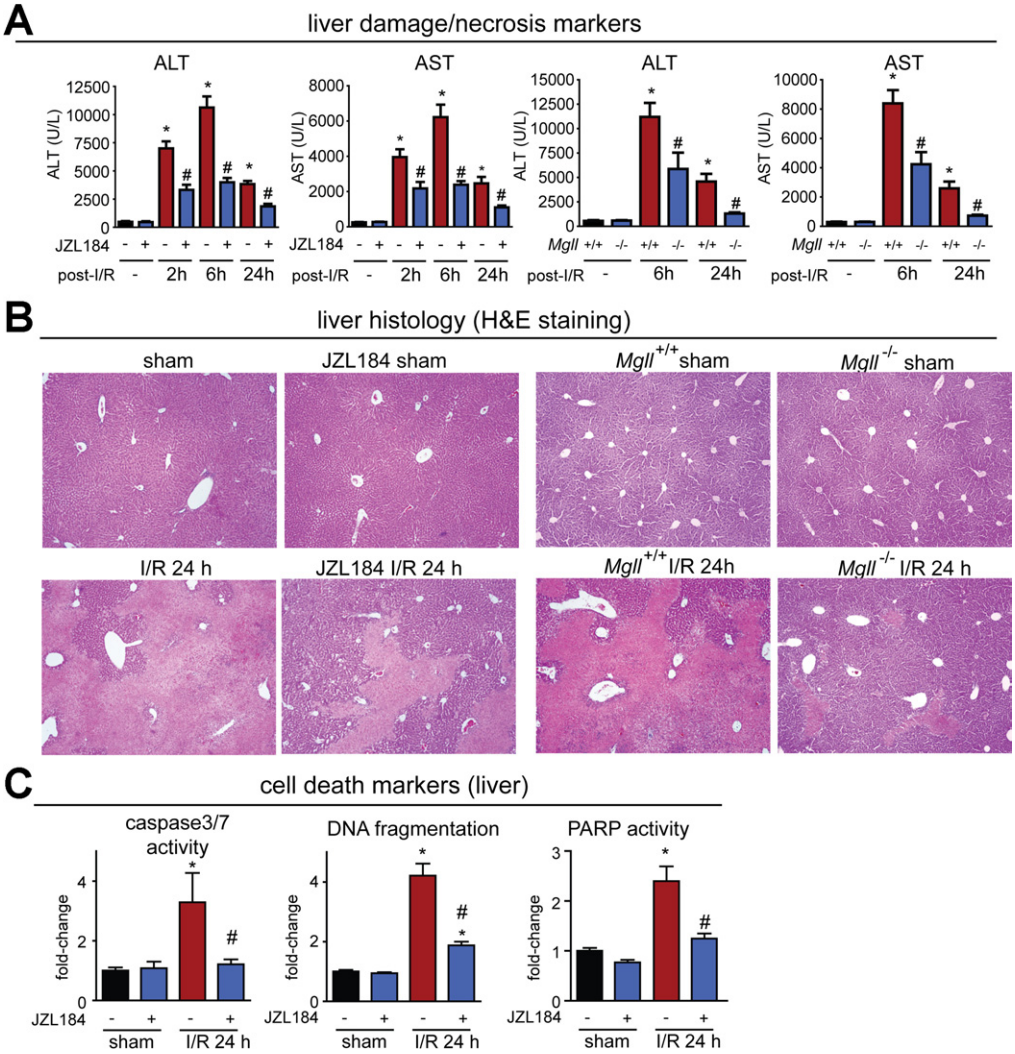

Figure 2. MAGL inactivation attenuates hepatic I/R-induced tissue injury. (*A*) Liver damage/necrosis markers ALT and AST are increased significantly in mouse plasma upon I/R induction 2, 6, and 24 hours after reperfusion, and both pharmacologic (JZL184, 40 mg/kg, IP) and genetic (*Mgll*$^{-/-}$) inactivation of MAGL substantially reduces these increased levels. (*B*) Liver histology (H&E staining) of mice subjected to sham surgery or 1 hour of ischemia followed by 24 hours of reperfusion (I/R 24 h) in vehicle vs JZL184-treated (40 mg/kg, IP, given before induction of ischemia) or in *Mgll*$^{+/+}$ vs *Mgll*$^{-/-}$ mice, showing representative images of coagulation necrosis (*lighter areas*) subjected to I/R that is attenuated significantly upon pharmacologic or genetic ablation of MAGL. (*C*) MAGL inhibition attenuates I/R-induced delayed cell death markers (caspase-3/-7 activity, DNA fragmentation, poly[adenosine diphosphate-ribose] polymerase activity [PARP]) after 24 hours of reperfusion (I/R 24 h). Data represent mean ± standard error of the mean of (*A*) 6–9 mice/group and (*C*) 5–11 mice/group. Significance is represented as (*A*) $^{*}P < .05$ between vehicle-treated I/R groups and sham vehicle-treated groups, and $^{\#}P < .05$ between JZL184-treated or *Mgll*$^{-/-}$ I/R groups and the corresponding I/R vehicle-treated or *Mgll*$^{+/+}$ groups; and (*C*) $^{*}P < .05$ between vehicle-treated I/R group and the sham groups, and $^{\#}P < .05$ between JZL184-treated I/R groups and vehicle-treated I/R groups.

found that MAGL inactivation significantly reduced inflammation, oxidative stress, and late apoptotic cell death (Figures 2*C*, 3*B*, 3*C*, and Supplementary Figure 4). Specifically, genetic and pharmacologic inactivation of MAGL markedly attenuated the infiltration of neutrophils evidenced by substantially lower myeloperoxidase staining (Figure 3*A*, Supplementary Figure 4*A*). Pharmacologic or genetic inactivation of MAGL also blocked I/R-induced acute early proinflammatory responses in cytokines TNF-α and interleukin 1β, chemokines macrophage inflammatory protein 1α and 2, and in hepatic expression of intercellular adhesion molecule 1 (Figure 3*B* and *C*, Supplementary Figure 4). The delayed oxidative stress induced by I/R, as measured by the lipid peroxidation marker 4-hydroxynonenal and the reactive oxygen species-generating nicotinamide adenine dinucleotide phosphate oxidase isoform 2 expression, also were reduced in MAGL-inactivated mice (Figure 3*B* and *C*, Supplementary Figure 4). Consistent with the hepatoprotection observed with both histologic evaluation and biochemistry (serum ALT/AST levels), we found that MAGL inactivation reduced both apoptotic (caspase-3 and caspase-7 activity and DNA fragmentation) and necrotic (poly[adenosine diphosphate-ribose] polymerase activity) cell death markers (Figure 2*C*, Supplementary Figure 4).

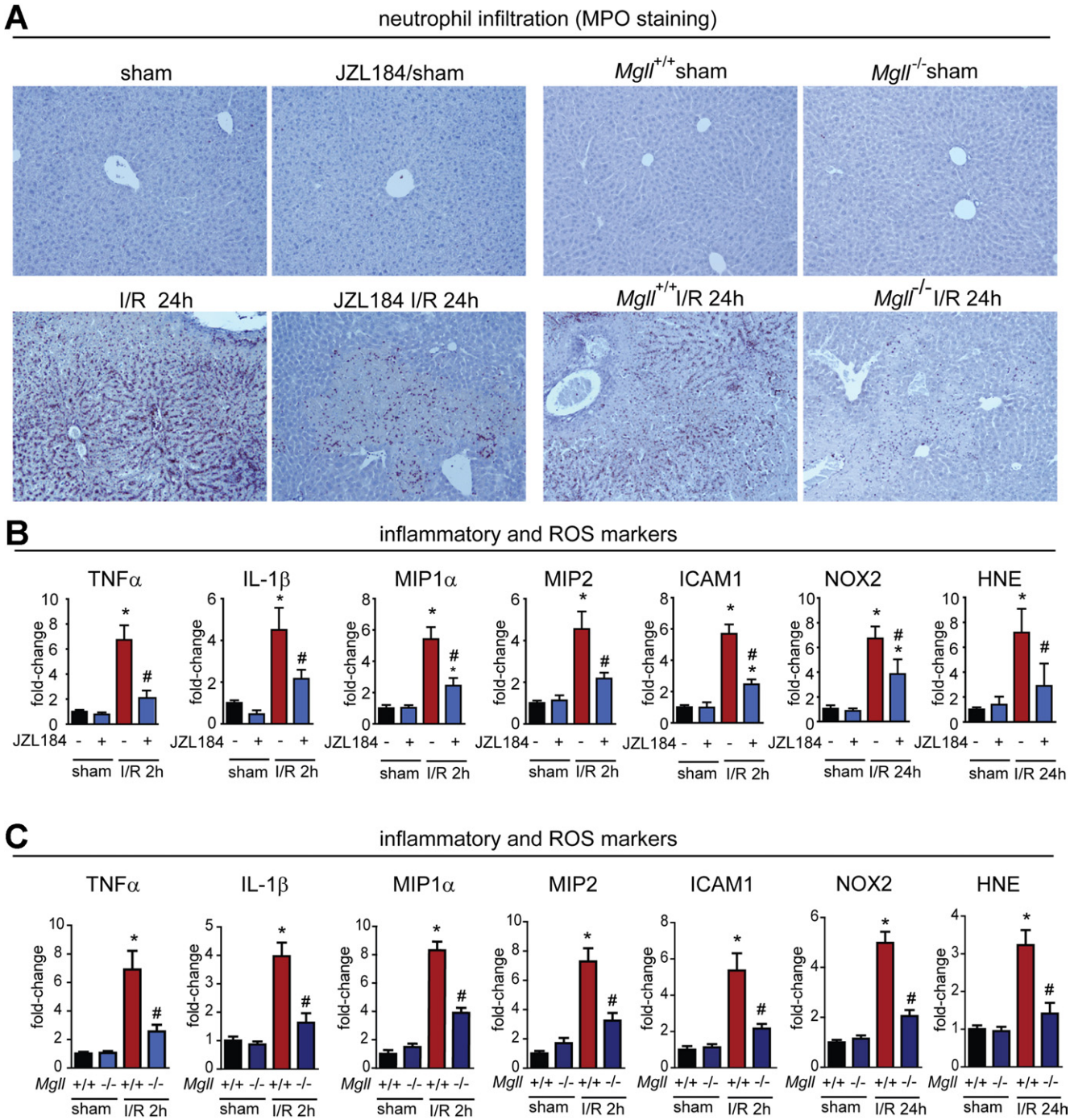

Figure 3. MAGL inactivation attenuates hepatic I/R-induced inflammation and oxidative stress. (*A*) Both pharmacologic and genetic blockade of MAGL causes massive delayed infiltration of neutrophils as assessed by myeloperoxidase (MPO) staining (*brown staining*) of livers after 24 hours of reperfusion after induction of 1 hour of hepatic ischemia (I/R 24 h). Representative images are shown. This neutrophil infiltration is attenuated significantly upon JZL184 treatment (40 mg/kg, IP) before ischemia or in $Mgll^{-/-}$ mice. (*B*) The I/R-induced early increases in proinflammatory cytokines, chemokines TNF-α, interleukin-1β, chemokines macrophage inflammatory protein (MIP1-α) and MIP-2, and adhesion molecule intercellular adhesion molecule 1 (ICAM-1) assessed after 2 hours of reperfusion (I/R 2 h) as well as the late oxidative stress markers nicotinamide adenine dinucleotide phosphate oxidase isoform 2 (NOX2) and 4-hydroxynonenal (HNE) assessed after 24 hours of reperfusion (I/R 24 h), are attenuated significantly upon JZL184 treatment (40 mg/kg, IP, before induction of ischemia) as well as in $Mgll^{-/-}$ I/R groups (*C*). Data represent mean ± standard error of the mean of 6–12 mice/group. Significance is represented as $^{*}P < .05$ between the indicated groups and the sham surgery vehicle-treated groups or sham $Mgll^{+/+}$ groups; $^{\#}P < .05$ vs the corresponding I/R vehicle-treated groups or $Mgll^{+/+}$ groups.

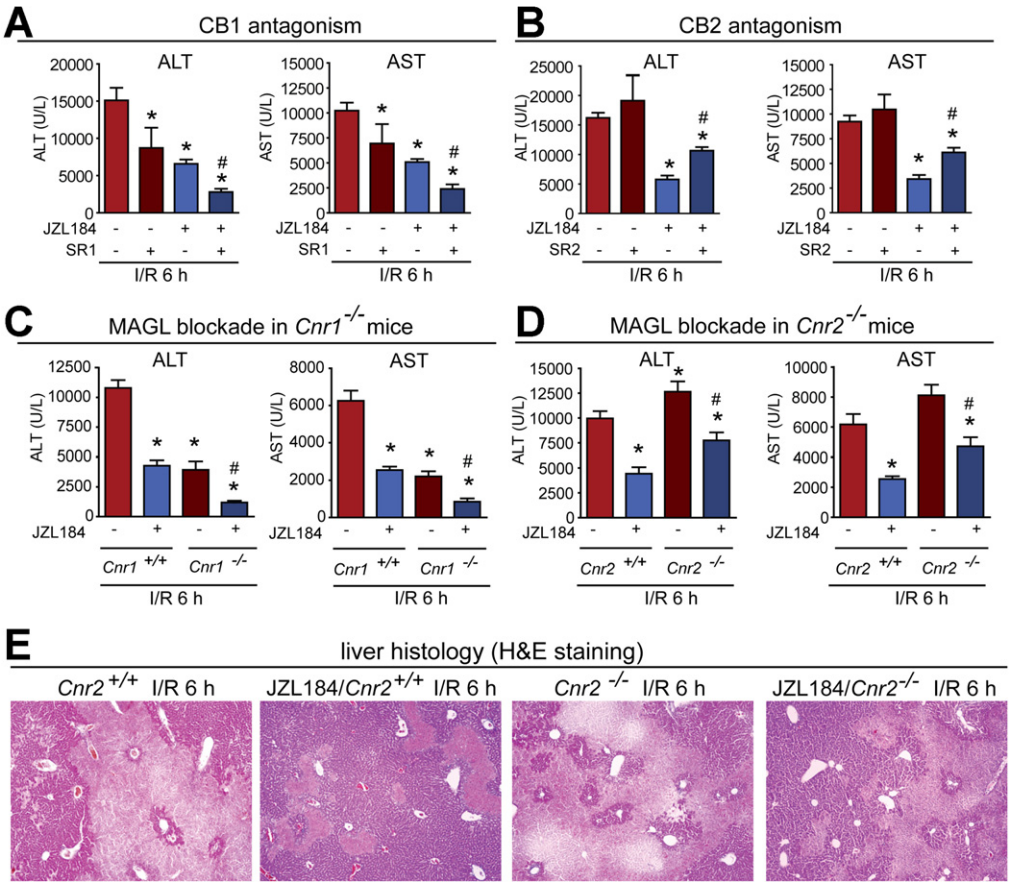

Figure 4. Hepatoprotective effects conferred by MAGL are partially owing to CB_2, but not CB_1 signaling. (*A* and *B*) The effect of the CB_1- and CB_2-receptor antagonists (*A*) SR141716A and (*B*) SR14452 on ALT and AST levels after 6 hours of reperfusion (I/R 6 h), respectively. SR141716A (3 mg/kg, IP) reduces ALT and AST levels in I/R mice, and this effect is additive when given in combination with JZL184 mice. SR14452 (3 mg/kg, IP) partially reverses the JZL184-induced reductions in ALT and AST levels. (*C* and *D*) Pharmacologic blockade of MAGL (JZL184, 40 mg/kg, IP) after 6 hours of reperfusion (I/R 6 h) exerts further decreases or attenuation of ALT and AST levels in (*C*) *Cnr1*$^{-/-}$ and (*D*) *Cnr2*$^{-/-}$ mice, respectively. (*E*) Liver histology (H&E staining) of *Cnr2*$^{+/+}$ or *Cnr2*$^{-/-}$ mice subjected to 1 hour of ischemia followed by 6 hours of reperfusion (I/R 6 h) or sham surgery in vehicle vs JZL184-treated (40 mg/kg, IP, given before induction of ischemia) mice, showing an attenuated hepatoprotective response to JZL184 in *Cnr2*$^{-/-}$ I/R mice compared with JZL184-treated *Cnr2*$^{+/+}$ mice. Data represent mean ± standard error of the mean of 6–12 mice/group. Significance is represented as $^{*}P < .05$ between (*A* and *B*) the indicated groups and vehicle-treated I/R group or (*C* and *D*) vehicle-treated *Cnr1*$^{+/+}$ or *Cnr2*$^{+/+}$ I/R groups, and $^{\#}P < .05$ between (*A* and *B*) SR141716A- or SR14452-treated JZL184-treated I/R groups or (*C* and *D*) JZL184-treated *Cnr1*$^{-/-}$ or *Cnr2*$^{-/-}$ I/R groups vs the corresponding JZL184-treated I/R groups or vehicle-treated *Cnr1*$^{-/-}$ or *Cnr2*$^{-/-}$ I/R groups, respectively.

Hepatoprotective Effects Conferred by MAGL Blockade Are Mediated Partially by Cannabinoid Receptor Type 2 but Not Receptor Type 1

We next tested whether the hepatoprotective effect induced by MAGL inactivation was owing to heightened cannabinoid signaling, suppressed eicosanoid production, or a mixture of both mechanisms. Consistent with a partial contribution by endocannabinoids, we found that the decreased levels of ALT and AST in JZL184-treated mice subjected to I/R were significantly, but not completely, reversed by the CB_2-receptor antagonist SR144528, and were not attenuated by the CB_1-receptor antagonist SR141716 (Figure 4*A* and *B*). As has been shown previously, SR141716 treatment reduced ALT and AST levels when given alone,[16] and exerted additive hepatoprotective effects when administered with JZL184 (Figure 4*A*). We observed similar results with JZL184 in *Cnr1*$^{-/-}$ and *Cnr2*$^{-/-}$ mice (Figure 4*C*–*E*). Our results thus show that the protective effects of MAGL blockade in I/R-induced liver injury are partly, but not completely, mediated by heightened endocannabinoid signaling acting on CB_2 receptors. Considering the observed reductions in liver eicosanoids in MAGL-disrupted mice, combined with past evidence supporting a protective effect of COX inhibitors in liver injury models, we put forth that MAGL blockade likely reduces I/R-induced liver damage by a dual mechanism involving both heightened endocannabinoid signaling and reduced eicosanoid production.

Cell-Type Specificity of Endocannabinoid and Eicosanoid Generation and Signaling

We next wanted to delve deeper into the specific cell types responsible for generating the endocannabinoids and eicosanoids, and to identify the target cells of these lipid signals. We first found that MAGL activity was substantially higher in isolated hepatocytes compared with NPCs (Supplementary Figure 6*A*). I/R-induced liver injury significantly increased the levels of 2-AG, AA, and

eicosanoids in hepatocytes but not in NPCs, showing that hepatic I/R promotes dysregulated endocannabinoid-eicosanoid metabolism primarily in hepatocytes (Supplementary Figure 6*B*). Although blocking MAGL in vivo increased 2-AG levels in both hepatocytes and NPCs, reductions in AA and eicosanoids only occurred in hepatocytes (Supplementary Figure 6*B–D*).

To investigate which cell types are affected by 2-AG signals, we used flow cytometry and quantitative polymerase chain reaction to show that CB_2 receptors are expressed primarily on Kupffer cells, endothelial cells, and neutrophils, but not on hepatocytes (Supplementary Figure 7). Consistent with this premise, we showed that MAGL blockade by JZL184, but not 2-AG, in isolated hepatocytes exposed to hypoxia-reoxygenation attenuated hepatocyte cell death as determined by reduced lactate dehydrogenase and ALT release in vitro (Supplementary Figure 8). However, 2-AG treatment of isolated Kupffer cells caused a partially CB_2-dependent reduction in TNFα levels in response to LPS stimulation (Supplementary Figure 9). In contrast, MAGL inhibition had no effect on LPS-induced TNFα release (data not shown). Collectively, our results indicate that both hepatocytes and nonparenchymal cells produce 2-AG that signals to CB_2 receptors on Kupffer cells, neutrophils, and endothelial cells, whereas eicosanoids primarily are generated by hepatocytes during hepatic I/R.

Inactivation of MAGL Exerts Hepatoprotective Effects Even When Administered After Reperfusion

We further asked if pharmacologic inhibition of MAGL is also protective when initiated after the induction of hepatic ischemia. Strikingly, we found that treatment with JZL184 (40 mg/kg, IP) even during the reperfusion period resulted in significant hepatoprotection when administered 1 and 3 hours after induction of hepatic reperfusion (Figure 5, Supplementary Figures 10 and 11). These provocative results suggest that MAGL inhibitors can protect against hepatic I/R injury when administered not only before but also after the liver is exposed to ischemic or hypoxic conditions.

Inactivation of MAGL Also Protects Liver Damage in Murine Hepatitis Models Induced by GalN/LPS or CCl_4

Finally, we tested whether inactivation of MAGL is also hepatoprotective in liver injury models caused by insults other than hepatic I/R. We found that MAGL blockade with JZL184 significantly protected mice against lethality caused by liver failure in the GalN/LPS model (83% lethality in vehicle-treated compared with 42% in JZL184-treated mice; $P = .04$ by the Fisher exact test). In nonlethal experiments, JZL184 pretreatment significantly reduces GalN/LPS-induced liver damage (Figure 6*A*). JZL184 pretreatment also effectively suppressed CCl_4-induced hepatic injury (Figure 6*B*). Consistent with the liver I/R model, MAGL inactivation by JZL184 also heightened

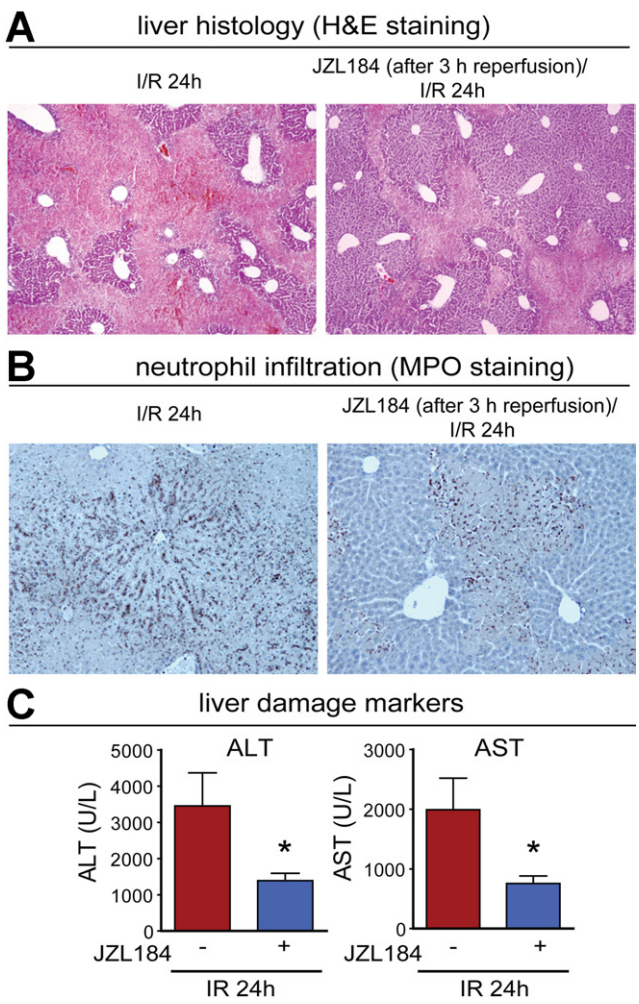

Figure 5. MAGL inhibition exerts hepatoprotection even when given after reperfusion. (*A*) Coagulation necrosis, (*B*) neutrophil infiltration, and (*C*) liver damage markers ALT and AST are reduced in hepatic I/R even when JZL184 is administered at 3 hours of reperfusion. All parameters were measured at 24 hours of reperfusion (24 h I/R). Data represent mean ± standard error of the mean of 6 mice/group. *$P < .05$ vs vehicle-treated I/R group.

2-AG signaling and attenuated the GalN/LPS and CCl_4-induced enhanced hepatic eicosanoid levels and liver injury (Supplementary Figure 12). MAGL inactivation by JZL184 significantly attenuated hepatic COX-2 mRNA, but not protein levels induced by GalN/LPS or CCl_4 (Supplementary Figure 13).

Discussion

There is increasing evidence suggesting that CB_2 stimulation by pharmacologic ligands may represent a promising treatment strategy for various liver diseases, as well as other disorders ranging from gastrointestinal, kidney, neurodegenerative, and autoimmune diseases, to pain and cancer.[8] Activation of CB_2 signaling affords protection in hepatic I/R by attenuation of acute proinflammatory responses orchestrated by activated endothelial and Kupffer cells, as well as by inhibition of delayed neutrophil infiltration and neutrophil-mediated liver injury.[8]

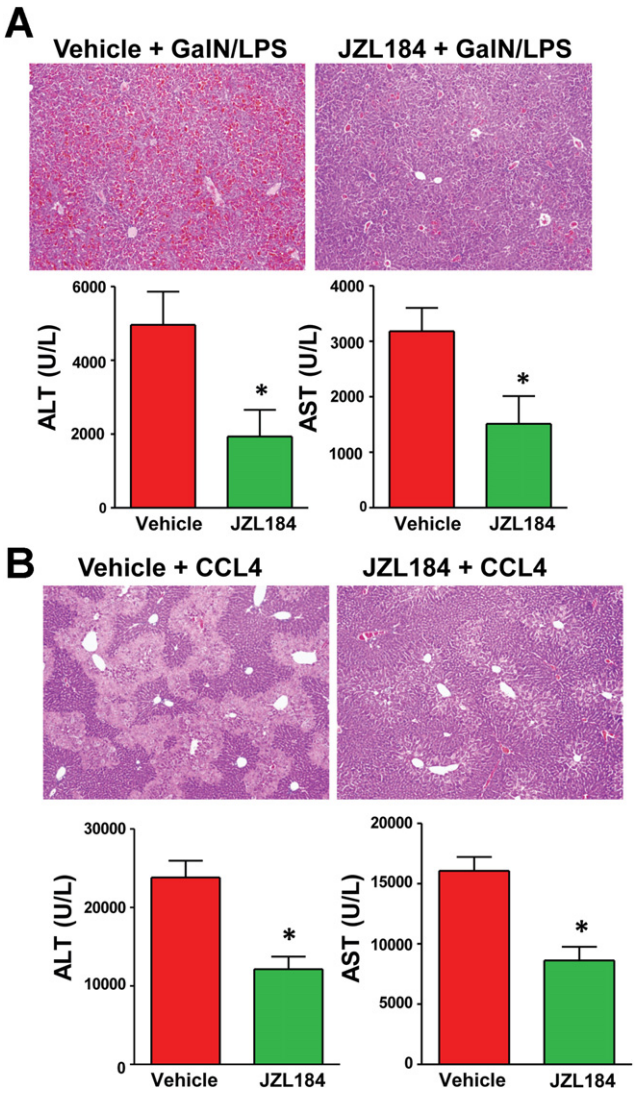

Figure 6. MAGL inactivation by JZL184 attenuates liver damage in acute murine liver injury models induced by GalN/LPS or CCl_4. Liver damage/necrosis markers ALT and AST are increased significantly in mouse serum upon treatment with (*A*) GalN/LPS for 7 hours (*lower panels*) or (*B*) CCl_4 for 24 hours (*lower panels*), and JZL184 (20 mg/kg, IP) pretreatment substantially reduces these increased enzyme levels. Liver histology (H&E staining, original magnification, 40×) showing representative images of liver tissue damage induced by (*A*) GalN/LPS (*upper panels*) or (*B*) CCl_4 (*upper panels*), which is significantly attenuated upon MAGL inhibition by JZL184. *$P < .05$ vs vehicle-treated control groups.

Pharmacologic or genetic inactivation of COX2 also has been shown to protect the liver against injury by suppressing inflammation and hepatocyte cell death.[21,22] We show here that MAGL blockade exerts hepatoprotective effects in multiple liver injury models through coordinately enhancing endocannabinoid CB_2 and lowering eicosanoid pathways, thereby limiting neutrophil infiltration and neutrophil-mediated liver damage. MAGL thus serves as a critical metabolic node that simultaneously controls 2 important lipid signaling pathways that limit liver injury.

We also provide compelling evidence for the intricate cell-to-cell communications of endocannabinoid and eicosanoid signals that contribute to the hepatoprotective effects conferred by MAGL inactivation. We show that endocannabinoids are generated by both hepatocytes and NPCs whereas eicosanoids primarily arise from hepatocytes. Consistent with previous reports, we also show that CB_2 receptors are not expressed on hepatocytes, but instead are localized to NPCs including Kupffer cells.[8] These results are corroborated further by our in vitro experiments showing that, in contrast to the inability to protect hepatocytes from hypoxia-induced cell death, 2-AG pretreatment significantly inhibits LPS-induced TNFα release from Kupffer cells. Our data are in agreement with a recently published study focusing on CB_2-mediated Kupffer cell polarization in alcohol-induced liver injury, which showed that Kupffer cells from CB_2-/- mice have enhanced LPS-stimulated TNFα induction whereas activation of CB_2 by JWH-133 inhibited TNFα production in LPS-treated RAW264.7 cells.[23] We also find that MAGL blockade reduces hepatic eicosanoid levels as early as 2 hours after reperfusion, before the infiltration of inflammatory cells into the liver, without any concordant changes in COX2 expression. These results show that the eicosanoid lowering effects of MAGL blockade likely are owing to reductions in the AA pool that generates eicosanoids rather than an indirect effect on COX2 expression. Second, these results suggest that the initial hepatoprotective effect is likely through reducing eicosanoids rather than enhancing endocannabinoids because the inflammatory immune cells that express CB_2 are not yet present 2 hours after reperfusion. These results are consistent with literature precedence showing the anti-inflammatory effect of CB_2 signaling in various immune and activated endothelial cells during I/R.[8] The earlier-mentioned previous results also are consistent with our data (not shown): the high-mobility group protein B1, released upon early hepatocellular necrosis during I/R to activate Kupffer and other inflammatory cells (eg, neutrophils) through Toll-like receptors, also substantially was reduced during I/R upon JZL184 treatment at an early time (2 h) of reperfusion (before neutrophil infiltration), coinciding with reduction of hepatic eicosanoid levels. However, we acknowledge that the interpretation derived from our cell-type specificity studies may be confounded by the procedures involved in isolating the individual cell types.

Although previous reports have shown that some eicosanoids such as prostaglandin E2 and prostacyclin analogs may be anti-inflammatory during liver inflammation given exogenously, lowering eicosanoids broadly by either genetic or pharmacologic blockade of COX2 also has been shown to be hepatoprotective in multiple other studies. We cannot rule out the possibility of other mechanisms involved in our hepatoprotective effects observed, such as the contribution of prostaglandin glyceryl esters or other potential biological active monoacylglycerols,[24] which also may modulate hepatic COX2 expression induced by various insults.[24] However, we believe that broadly lowering eicosanoids by MAGL inactivation causes an overall

net anti-inflammatory eicosanoid environment, much like that with COX inhibition, that is responsible, at least in part, for our hepatoprotective phenotypes in addition to heightened endocannabinoid signaling. We also cannot exclude the possibility that these eicosanoids, which have been shown to be both anti-inflammatory and proinflammatory, exert their biological effects in cell-type–, tissue-type–, and context-dependent manners.

One potential advantage of MAGL inhibitors over dual COX1/COX2 inhibitors and COX2-selective inhibitors is that MAGL only controls eicosanoid metabolism in specific tissues such as the brain, liver, and lung, but not, for example, in the gut.[14] Thus, MAGL blockade could avoid some of the mechanism-based gastrointestinal and cardiovascular side effects[25] associated with COX inhibition, and even may protect against COX inhibitor–induced gastrointestinal injury through endocannabinoid-dependent mechanisms.[14,26] Furthermore, because MAGL controls the AA precursor pools for general eicosanoid biosynthesis, MAGL inhibitors may have broader effects that extend beyond COX-mediated pathways (eg, CYP450-generated 5,6-epoxyeicosatrienoic acid). Although previous studies have shown that chronic and complete inhibition of MAGL results in desensitization of CB_1 signaling in the nervous system,[15,27] we show here that CB_2-mediated hepatoprotective effects still are maintained in MAGL-/- mice, indicating that immune cell CB_2 function does not become desensitized under chronic MAGL ablation. Although the studies described here all used acute liver injury models, it will be important to consider any potential adverse effects that may arise from brain CB_1 desensitization in any future therapies that require chronic MAGL inhibitor dosing.

In contrast to CB_2 signaling, which attenuates hepatic injury, fibrosis, and promotes regeneration,[5,23,28] CB_1 signaling contributes to increased damage and fibrosis in multiple liver pathologies where CB_1 inhibition is protective.[11,13] Previous studies also have shown hepatoprotective effects of CB_1 antagonists in I/R.[9,16] In this study, we show that MAGL inhibitors, similarly to direct CB_2 agonists, can be combined efficiently with CB_1 antagonists to achieve even greater benefits. This also indicates that the enhanced 2-AG signaling conferred by MAGL blockade is selectively stimulating CB_2 but not CB_1 to exert hepatoprotective effects, and forecasts a potential therapeutic utility of the combination of MAGL inhibitors with peripherally restricted CB_1 antagonists that would avoid the central anxiety and depression effects that halted the clinical development of global CB_1 antagonists.[12]

Despite the fact that hepatic I/R, as well as I/R injury of other organs, is a common complication of many diseases and surgical procedures, there is currently a remarkable lack of pharmacologic therapies to provide improved outcomes and avoid organ failure and death. In this study, we found that pharmacologic inhibition of MAGL either before or after the initiation of hepatic I/R confers substantial protection against the inflicted injury. We therefore put forth MAGL and its inhibitors as a novel next-generation therapeutic strategy toward not only preventing, but also treating, I/R injury, in the hope of improving the outcome of diseases and surgeries that expose the liver to hypoxia, inflammation, and oxidative stress. Importantly, we also show that MAGL inactivation by JZL184 is similarly effective in protecting GalN/LPS- and CCl_4-induced acute liver injury, indicating that MAGL inhibitors may have broader utility beyond conditions that cause hepatic I/R. Because the mechanisms underlying these tissue injuries share lots of similarities across other organs,[29] generally involving damage through inflammation and oxidative stress, we anticipate that MAGL inhibitors may exert beneficial effects in other pathologies (eg, myocardial infarction, stroke, whole-body ischemia associated with various forms of shock, and so forth) where either CB_2 agonists or COX inhibitors have both shown efficacy.[30–34]

Supplementary Material

Note: To access the supplementary material accompanying this article, visit the online version of *Gastroenterology* at www.gastrojournal.org, and at http://dx.doi.org/10.1053/j.gastro.2012.12.028.

References

1. Pacher P, Hasko G. Endocannabinoids and cannabinoid receptors in ischaemia-reperfusion injury and preconditioning. Br J Pharmacol 2008;153:252–262.
2. Walsh KB, Toledo AH, Rivera-Chavez FA, et al. Inflammatory mediators of liver ischemia-reperfusion injury. Exp Clin Transplant 2009;7:78–93.
3. Horvath B, Magid L, Mukhopadhyay P, et al. A new cannabinoid CB2 receptor agonist HU-910 attenuates oxidative stress, inflammation and cell death associated with hepatic ischaemia/reperfusion injury. Br J Pharmacol 2012;165:2462–2478.
4. Kobayashi M, Takeyoshi I, Kurabayashi M, et al. The effects of a cyclooxygenase-2 inhibitor, FK3311, on total hepatic ischemia-reperfusion injury of the rat. Hepatogastroenterology 2007;54:522–526.
5. Batkai S, Osei-Hyiaman D, Pan H, et al. Cannabinoid-2 receptor mediates protection against hepatic ischemia/reperfusion injury. FASEB J 2007;21:1788–1800.
6. Hamada T, Tsuchihashi S, Avanesyan A, et al. Cyclooxygenase-2 deficiency enhances Th2 immune responses and impairs neutrophil recruitment in hepatic ischemia/reperfusion injury. J Immunol 2008;180:1843–1853.
7. Yokoyama Y, Nimura Y, Nagino M, et al. Role of thromboxane in producing hepatic injury during hepatic stress. Arch Surg 2005;140:801–807.
8. Pacher P, Mechoulam R. Is lipid signaling through cannabinoid 2 receptors part of a protective system? Prog Lipid Res 2011;50:193–211.
9. Caraceni P, Pertosa AM, Giannone F, et al. Antagonism of the cannabinoid CB-1 receptor protects rat liver against ischaemia-reperfusion injury complicated by endotoxaemia. Gut 2009;58:1135–1143.
10. Jeong WI, Osei-Hyiaman D, Park O, et al. Paracrine activation of hepatic CB1 receptors by stellate cell-derived endocannabinoids mediates alcoholic fatty liver. Cell Metab 2008;7:227–235.
11. Teixeira-Clerc F, Julien B, Grenard P, et al. CB1 cannabinoid receptor antagonism: a new strategy for the treatment of liver fibrosis. Nat Med 2006;12:671–676.

12. Kunos G, Tam J. The case for peripheral CB(1) receptor blockade in the treatment of visceral obesity and its cardiometabolic complications. Br J Pharmacol 2011;163:1423–1431.
13. Tam J, Liu J, Mukhopadhyay B, et al. Endocannabinoids in liver disease. Hepatology 2011;53:346–355.
14. Nomura DK, Morrison BE, Blankman JL, et al. Endocannabinoid hydrolysis generates brain prostaglandins that promote neuroinflammation. Science 2011;334:809–813.
15. Schlosburg JE, Blankman JL, Long JZ, et al. Chronic monoacylglycerol lipase blockade causes functional antagonism of the endocannabinoid system. Nat Neurosci 2010;13:1113–1119.
16. Batkai S, Mukhopadhyay P, Horvath B, et al. Delta8-tetrahydrocannabivarin prevents hepatic ischaemia/reperfusion injury by decreasing oxidative stress and inflammatory responses through cannabinoid CB2 receptors. Br J Pharmacol 2012;165:2450–2461.
17. Cao Z, Yuan Y, Jeyabalan G, et al. Preactivation of NKT cells with alpha-GalCer protects against hepatic ischemia-reperfusion injury in mouse by a mechanism involving IL-13 and adenosine A2A receptor. Am J Physiol Gastrointest Liver Physiol 2009;297:G249–G258.
18. Cao Z, Dhupar R, Cai C, et al. A critical role for IFN regulatory factor 1 in NKT cell-mediated liver injury induced by alpha-galactosylceramide. J Immunol 2010;185:2536–2543.
19. Liu W, Hou Y, Chen H, et al. Sample preparation method for isolation of single-cell types from mouse liver for proteomic studies. Proteomics 2011;11:3556–3564.
20. Long JZ, Li W, Booker L, et al. Selective blockade of 2-arachidonoylglycerol hydrolysis produces cannabinoid behavioral effects. Nat Chem Biol 2009;5:37–44.
21. Begay CK, Gandolfi AJ. Late administration of COX-2 inhibitors minimize hepatic necrosis in chloroform induced liver injury. Toxicology 2003;185:79–87.
22. Han C, Li G, Lim K, et al. Transgenic expression of cyclooxygenase-2 in hepatocytes accelerates endotoxin-induced acute liver failure. J Immunol 2008;181:8027–8035.
23. Louvet A, Teixeira-Clerc F, Chobert MN, et al. Cannabinoid CB2 receptors protect against alcoholic liver disease by regulating Kupffer cell polarization in mice. Hepatology 2011;54:1217–1226.
24. Rouzer CA, Marnett LJ. Endocannabinoid oxygenation by cyclooxygenases, lipoxygenases, and cytochromes P450: cross-talk between the eicosanoid and endocannabinoid signaling pathways. Chem Rev 2011;111:5899–5921.
25. Dajani EZ, Islam K. Cardiovascular and gastrointestinal toxicity of selective cyclo-oxygenase-2 inhibitors in man. J Physiol Pharmacol 2008;59(Suppl 2):117–133.
26. Kinsey SG, Nomura DK, O'Neal ST, et al. Inhibition of monoacylglycerol lipase attenuates nonsteroidal anti-inflammatory drug-induced gastric hemorrhages in mice. J Pharmacol Exp Ther 2011;338:795–802.
27. Chanda PK, Gao Y, Mark L, et al. Monoacylglycerol lipase activity is a critical modulator of the tone and integrity of the endocannabinoid system. Mol Pharmacol 2010;78:996–1003.
28. Julien B, Grenard P, Teixeira-Clerc F, et al. Antifibrogenic role of the cannabinoid receptor CB2 in the liver. Gastroenterology 2005;128:742–755.
29. Eltzschig HK, Eckle T. Ischemia and reperfusion—from mechanism to translation. Nat Med 2011;17:1391–1401.
30. Maheshwari A, Badgujar L, Phukan B, et al. Protective effect of etoricoxib against middle cerebral artery occlusion induced transient focal cerebral ischemia in rats. Eur J Pharmacol 2011;667:230–237.
31. Zarruk JG, Fernandez-Lopez D, Garcia-Yebenes I, et al. Cannabinoid type 2 receptor activation downregulates stroke-induced classic and alternative brain macrophage/microglial activation concomitant to neuroprotection. Stroke 2012;43:211–219.
32. Defer N, Wan J, Souktani R, et al. The cannabinoid receptor type 2 promotes cardiac myocyte and fibroblast survival and protects against ischemia/reperfusion-induced cardiomyopathy. FASEB J 2009;23:2120–2130.
33. Tuma RF, Steffens S. Targeting the endocannabiniod system to limit myocardial and cerebral ischemic and reperfusion injury. Curr Pharm Biotechnol 2012;13:46–58.
34. Montecucco F, Lenglet S, Braunersreuther V, et al. CB(2) cannabinoid receptor activation is cardioprotective in a mouse model of ischemia/reperfusion. J Mol Cell Cardiol 2009;46:612–620.

Received August 2, 2012. Accepted December 30, 2012.

Reprint requests

Address requests for reprints to: Pál Pacher, MD, PhD, National Institute on Alcohol Abuse and Alcoholism, National Institutes of Health, 5625 Fishers Lane, MSC-9413, Room 2N-17, Rockville, Maryland 20852. e-mail: pacher@mail.nih.gov; fax: (301) 480-0257.

Acknowledgments

The authors are indebted to Dr George Kunos, the Scientific Director of the National Institute on Alcohol Abuse and Alcoholism, for continuous support.

Conflicts of interest

These authors disclose the following: Daniel Nomura and Benjamin Cravatt have filed a patent (US patent application serial no. 12/998,642) "Methods and compositions related to targeting monoacylglycerol lipase," which relates to inhibitors of monoacylglycerol lipase and associated methods, compositions, and potential uses for treating human disorders that are associated with endocannabinoid signaling. The remaining authors disclose no conflicts.

Funding

Supported by the Intramural Program of the National Institutes of Health/National Institute on Alcohol Abuse and Alcoholism (P.P.), University of California Berkeley/Department of Nutritional Sciences and Toxicology start-up funds (D.K.N., M.M.M.), National Institute on Drug Abuse (R00DA030908 to D.K.N. and M.M.M., and DA017259 to B.F.C.), and the Skaggs Institute for Chemical Biology (B.F.C.).

Supplementary Materials and Methods

Induction of Hepatic I/R

Briefly, male C57BL/6 mice were anesthetized with ketamine (100 mg/kg) and xylazine (10 mg/kg). The liver was exposed by midline laparotomy, and the hepatic hilum was carefully dissected and an atraumatic vascular clamp was applied to the hepatic artery and the portal vein branches that supply the median and left lateral lobes of the liver. The abdomen was covered with a piece of saline-soaked gauze to prevent dehydration, and the mice were placed on a heating pad to prevent drop of core temperature. The duration of hepatic ischemia was 60 minutes, after which the vascular clamp was removed to initiate hepatic reperfusion and the abdominal wall was sutured; the animals were returned to their cages, which were kept on a heating pad. After completion of reperfusion for 2, 6, or 24 hours, the mice were anesthetized with isoflurane inhalation, the abdomens and thoraxes were opened, and whole blood samples were collected by cardiac puncture before removal of the ischemic liver lobes for histologic and biochemical analysis. Sham surgeries were performed by following a similar procedure but without vascular occlusion.

Measurement of Endocannabinoids and Eicosanoids

Livers or isolated cells were homogenized in 1:1 hexane/ethyl acetate (3 mL) and phosphate-buffered saline (1 mL) in the presence of internal standards, 10 pmol d_9-PGE_2, 10 nmol pentadecanoic acid, 10 nmol d_5-2-AG, and 10 pmol d_4-anandamide. The organic layer was extracted and dried under N_2 and resuspended in 120 μL of chloroform. An aliquot (10 μL) was injected onto an Agilent 6430 QQQ-LC/MS/MS (Santa Clara, CA) and metabolite levels were quantified based on preestablished single reaction monitoring methods[1] and integrating the area under the curve, compared with internal standard, normalized to wet tissue weight.

Metabolite separation by liquid chromatography for lipophilic metabolites was achieved using a Gemini reverse-phase C18 column (50 mm $\times$ 4.6 mm with 5-μm-diameter particles) from Phenomonex (Torrance, CA). For liquid chromatography separation of lipid metabolites, mobile phase A consisted of 95:5 water/methanol and mobile phase B consisted of 60:35:5 isopropanol/methanol/water. Formic acid (0.1%) or ammonium hydroxide (0.1%) was included to assist in ion formation in positive ionization and negative ionization modes, respectively. For 2-AG and anandamide measurements, the flow rate for each run started at 0.1 mL/min with 0% B. At 5 minutes, the solvent was immediately changed to 60% B with a flow rate of 0.4 mL/min and increased linearly to 100% B over 15 minutes. This was followed by an isocratic gradient of 100% B for 8 minutes at 0.5 mL/min before equilibrating for 3 minutes at 0% B at 0.5 mL/min. For targeted eicosanoid and fatty acid, the flow rate for each run started at 0.1 mL/min with 0% B. At 3 minutes, the flow rate was increased to 0.4 mL/min with a linear increase of solvent B to 100% over 17 minutes. This was followed by an isocratic gradient of 100% B for 7 minutes at 0.5 mL/min before equilibrating for 3 minutes at 0% B at 0.5 mL/min.

The following mass spectrometry parameters were used to measure the indicated metabolites (precursor ion, product ion, collision energy in V, polarity): AEA (348, 62, 11, positive), *d*4-AEA (352, 66, 11, positive), C20:4 MAG or 2-AG (379, 287, 8, positive), d5-2-AG (384, 287, 8, positive), pentadecanoic acid (241, 241, 0, negative), AA (303, 303, 0, negative), PGE_2 (351, 271, 10, negative), PGD_2 (351, 271, 10, negative), $PGF_{2\alpha}$ (353, 193, 20, negative), TXB2 (369, 195, 5, negative), and 6-keto-$PGF_{1\alpha}$ (369, 163, 20, negative). Mass spectrometry analysis was performed with an electrospray ionization source. The drying gas temperature was 350°C, the drying gas flow rate was 11 L/min, and the nebulizer pressure was 35 psi. Metabolites targeted by single reaction monitoring were quantified by measuring the area under the peak in comparison to the internal standards. For metabolites for which isotopic internal standards were not used, external standard curves with the internal standard vs metabolite standard were generated.

Isolation of Hepatocytes, NPCs, and KCs From Mouse Liver

Mice were anesthetized by isoflurane inhalation, the abdomens were opened, and the portal vein was exposed. The liver was perfused in situ via the portal vein using 50 mL of an ethylene glycol-bis(β-aminoethyl ether)-*N,N,N′,N′*-tetraacetic acid (EGTA) buffer through a 22-gauge intravenous catheter. The liver was then perfused with 50 mL of 0.075% type IV collagenase in Gey's balanced salt solution (Sigma Chemical Co, St Louis, MO). The liver was removed and diced into small pieces and then digested in 0.009% collagenase solution for 30 minutes at 37°C with constant stirring. The crude cell suspension was filtered through a nylon mesh (0.1 mm) to remove debris and connective tissue. The cell suspension was then centrifuged at 50*g* for 5 minutes to pellet the hepatocytes, and the supernatant was recovered for purification of NPCs.

The hepatocyte pellets were washed twice with a hepatocyte washing medium (Invitrogen, Grand Island, NY) and were further purified by centrifugation on 10% OptiPrep at 50*g* for 10 minutes. The viable parenchymal cells were collected and washed 2 more times and were resuspended in a complete culture medium (Dulbecco's modified Eagle medium [DMEM] supplemented with 10% fetal bovine serum and 1% penicillin/streptomycin).

The NPC-containing supernatants were centrifuged at 50*g* for 3 minutes twice to eliminate residual hepatocytes. The supernatant was then centrifuged at 300*g*

for 10 minutes, and the resulting pellets were incubated with a red blood cell lysis buffer (eBioscience, San Diego, CA) to remove red blood cells. After washing twice in a washing solution (PBS supplemented with 2% fetal bovine serum and 2 mmol/L EDTA), the cells were resuspended in 37% Percoll (GE Healthcare Bio-Sciences, Uppsala, Sweden) and were then gently overlayed onto 70% Percoll and centrifuged for 25 minutes at 800*g*. Purified NPCs were collected from the interface and washed twice in the washing buffer. For purification of KCs, the NPCs were stained with a phycoerythrin (PE)-conjugated anti-F4/80 antibody and were then incubated with anti-PE microbeads (Miltenyi Biotec, Auburn, CA). KCs were separated using the MACS system (Miltenyi Biotec) as the column-bound cells, and the elution fraction was also collected that contained NPCs with KCs depleted.

Hypoxia-Reoxygenation Treatment of Isolated Mouse Hepatocytes

The isolated hepatocytes were seeded at a density of 0.5×10^6 cells per well in 6-well plastic plates coated with collagen I (Becton Dickinson Labware, Bedford, MA) and were cultured in DMEM (Gibco, Grand Island, NY) supplemented with 10% fetal bovine serum in a humidified atmosphere of 5% CO_2/95% air at 37°C. On the following day, the cells were changed to DMEM supplemented with 5% fetal bovine serum and were treated with various concentrations of 2-AG or JZL184 for 4 hours. The cells were then subjected to a hypoxic condition, which was attained by flushing a hypoxia chamber (Billups-Rothenberg, Del Mar, CA) with a gas mixture of 94% N_2/5% CO_2/1% O_2 for 3 minutes. Following 12 hours of hypoxia, reoxygenation of hepatocytes was initiated by opening the chamber and placing the cells back to normoxia culture condition for an additional 12 hours.

Determination of Apoptotic Hepatic Cell Death

Caspase-3/7 activity in hepatic tissue lysates was measured using the Apo-One Homogenous Caspase-3/7 Assay Kit (Promega Corp, Madison, WI). An aliquot of caspase reagent was added to each well and mixed on a plate shaker for 1 hour at room temperature shielded from light, and the fluorescence was measured. The quantitative determinations of cytoplasmic histone-associated DNA fragmentation (mononucleosomes and oligonucleosomes) due to cell death in liver homogenates were measured using an enzyme-linked immunosorbent assay (ELISA) kit (Roche Diagnostics GmbH, Mannheim, Germany). PARP activities in the liver homogenates were performed using the universal colorimetric assay kit (Trevigen Inc, Gaithersburg, MD) based on determination of the biotinylated poly (ADP-ribose) incorporation onto the histone proteins coated in ELISA wells.

Real-Time Polymerase Chain Reaction Analyses of mRNA Levels of Inflammatory Markers and COX-2

Total RNA was isolated from liver homogenate using TRIzol reagent (Invitrogen, Carlsbad, CA) according to the manufacturer's instructions. The isolated RNA was treated with ribonuclease-free deoxyribonuclease (Ambion, Austin, TX) to remove traces of genomic DNA contamination. One microgram of total RNA was reverse transcribed to complementary DNA using SuperScript II (Invitrogen). The target gene expression was quantified with Power SYBR Green PCR Master Mix using an ABI HT7900 real-time polymerase chain reaction (PCR) instrument (Applied Biosystems, Foster City, CA). Each amplified sample in all wells was analyzed for homogeneity using dissociation curve analysis. After denaturation at 95°C for 2 minutes, 40 cycles were performed at 95°C for 10 seconds and at 60°C for 30 seconds. Relative quantification was calculated using the comparative CT method ($2 - \Delta\Delta Ct$ method: $\Delta\Delta Ct = \Delta Ct$ sample $- \Delta Ct$ reference). Lower ΔCT values and lower $\Delta\Delta CT$ reflect a relatively higher amount of gene transcript. Statistical analyses were performed for at least 6 to 15 replicate experimental samples in each set. Primers used were as follows: MIP1-α, 5′-TGCCCTTGCTGTTCTTCTCTG-3′ and 5′-CAACGATGAATTGGCGTGG-3′; MIP2, 5′-AGTGAACTGCGCTGTCAATGC-3′ and 5′-AGGCAAACTTTTTGACCGCC-3′; TNF-α, 5′-AAGCCTGTAGCCCACGTCGTA-3′ and 5′-AGGTACAACCCATCGGCTGG-3′; ICAM-1, 5′-AACTTTTCAGCTCCGGTCCTG-3′ and 5′-TCAGTGTGAATTGGACCTGCG-3′; COX-2, 5′-CTCAATGAGTACCGCAAACGC3′ and 5′-TGGACGAGGTTTTTCCACCAG-3′; actin, 5′-TGCACCACCAACTGCTTAG-3′ and 5′-GGATGCAGGGATGATGTTC-3′.

Western Blotting Analysis of COX-2 Expression

Liver tissues were homogenized in a mammalian tissue protein extraction reagent (Pierce, Rockford, IL) supplemented with protease and phosphatase inhibitors (Roche Diagnostics). Aliquots of 50 μg of protein samples were fractionated by sodium dodecyl sulfate/polyacrylamide gel electrophoresis, transferred to a nitrocellulose membrane, and subjected to immunoblotting using a primary anti–COX-2 antibody at 1:1000 dilution (Santa Cruz Biotechnology, Santa Cruz, CA). After subsequent washing with PBS-Tween, the membranes were probed with appropriate secondary antibodies conjugated with horseradish peroxidase (Pierce). Then the membranes were developed using a SuperSignal West Pico Chemiluminescent Substrate Detection Kit (Pierce). To confirm uniform loading, membranes were stripped and reprobed with a β-actin antibody (Chemicon, Ramona, CA).

Measurement of Hepatic 4-Hydroxynonenal Content

Lipid peroxides are unstable indicators of oxidative stress in cells that decompose to form more complex and reactive compounds such as 4-hydroxynonenal (HNE), which has been shown to be capable of binding to proteins and forming stable HNE adducts. HNE in the hepatic tissues was determined using a kit (Cell Biolabs, San Diego, CA). In brief, bovine serum albumin or hepatic tissue extracts (10 μg/mL) were adsorbed onto a 96-well plate for 12 hours at 4°C. HNE adducts present in the sample or standard were probed with an anti-HNE antibody, followed by a horseradish peroxidase–conjugated secondary antibody. The contents of HNE-protein adducts in the unknown samples were determined by comparing with a standard curve.

Real-Time PCR Analysis of CB_2 Receptor Expression

Total RNA was isolated from whole liver tissue or isolated liver cellular subpopulations using TRIzol (Invitrogen) according to the manufacturer's instructions. The concentration and purity of the isolated RNA were measured spectrophotometrically at 260 nm and 280 nm. A total of 2 μg of RNA was treated with 2 U of deoxyribonuclease I (Thermo Scientific, Hudson, NH) at 37°C for 30 minutes. The reaction was stopped by adding 2 mmol/L EDTA followed by heat inactivation at 65°C for 10 minutes. Reverse transcription was performed using a High Capacity cDNA Reverse Transcription Kit (Applied Biosystems, Grand Island, NY) following the manufacturer's instructions. The reverse-transcription product was 10-fold diluted in nuclease-free water for real-time PCR reaction. Quantitative real-time PCR analysis was performed using a 7500 Real Time QPCR Detector System with Power SYBR Green qPCR Master Mix (Applied Biosystems) according to the manufacturer's instructions. The following primers were used for the reaction: CB_2 forward 5′-GCCCGAGTCAGAAGTCCGTTC-3′, reverse 5′-GCCACCTTCCAGCCAACCAGC-3′.

Flow Cytometry

The surface expression of CB_2 receptors was determined using the flow cytometry technique. To rule out the potential cross reaction with immunoglobulin receptor (FcgII, CD32) while determining the surface expression of CB_2 receptors in spleen and liver NPCs, the cells were blocked with CD32 antibody (5 mg/mL; BD Biosciences, San Jose, CA) for 15 minutes followed by incubation with CB_2 antibody/fluorescein isothiocyanate (Cayman, Ann Arbor, MI) and immune cell-specific antibodies in compatible color combination, including CD4-PE (BD Biosciences), Gr1.1-PE (Invitrogen), F4/80-APC (eBioscience), NK1.1-APC (eBioscience), and CD19-APC (eBioscience) for 1 hour on ice. Cells were analyzed using a FACSCalibur flow cytometer (BD Biosciences) with the Cell Quest Program.

Supplementary Reference

1. Nomura DK, Morrison BE, Blankman JL, et al. Endocannabinoid hydrolysis generates brain prostaglandins that promote neuroinflammation. Science 2011;334:809–813.

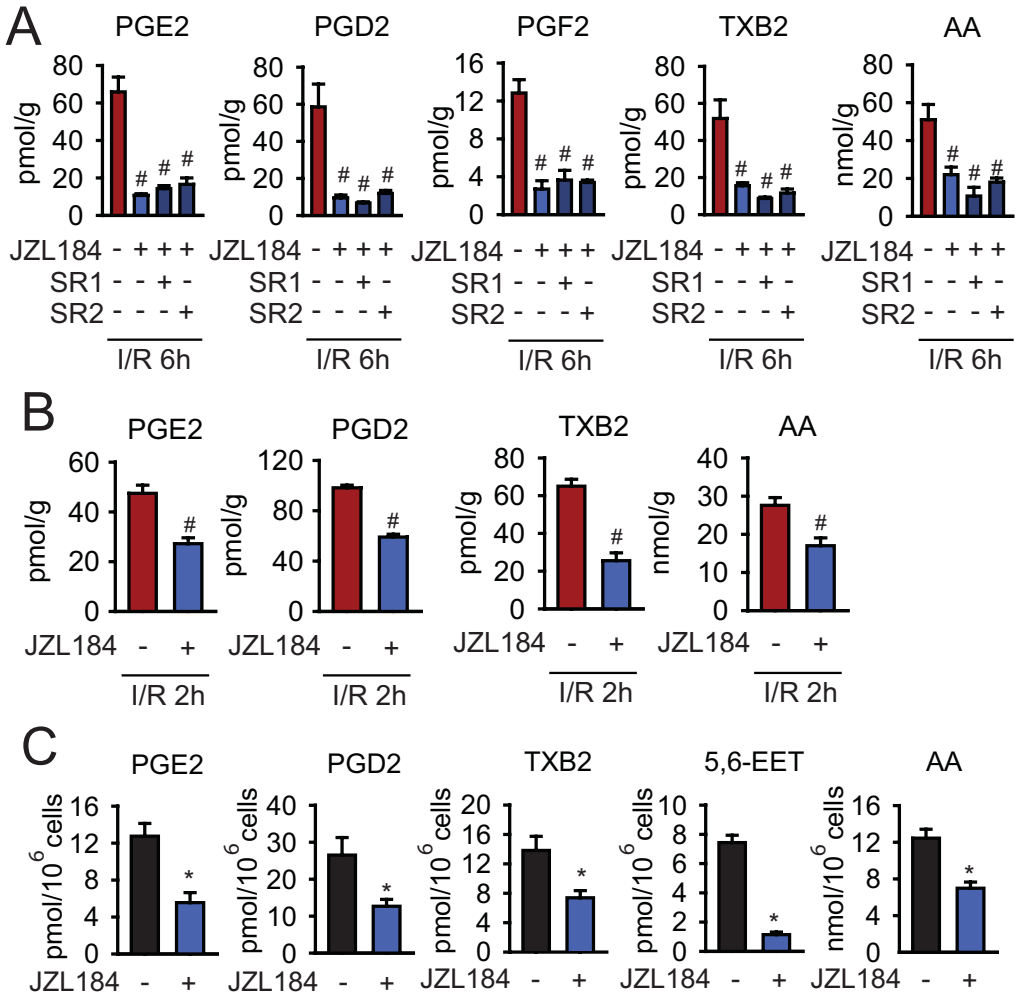

Supplementary Figure 1. MAGL blockade reduces the AA precursor pool for eicosanoid biosynthesis. (*A*) MAGL inactivation reduces AA and eicosanoids in the sham or I/R livers, measured after 6 hours of reperfusion. The reductions in eicosanoids are not attenuated on coadministration of CB_1 or CB_2 antagonists SR141716A (SR1) or SR14452 (SR2) (3 mg/kg IP), respectively, with JZL184. JZL184 (40 mg/kg IP) was given 1 hour before inducing ischemia in the liver, and endocannabinoid and eicosanoid levels were measured after 6 hours of reperfusion after ischemia by single reaction monitoring–based liquid chromatography/tandem mass spectrometry (LC-MS/MS) analysis. (*B*) MAGL blockade (JZL184, 40 mg/kg IP, 1 hour before ischemia) reduces AA and eicosanoids in I/R livers, measured after 2 hours of reperfusion. (*C*) Basal liver eicosanoid levels are lowered on chronic MAGL blockade with JZL184 (40 mg/kg IP, once per day treatment over 5 days, with livers removed 4 hours after final treatment). Data represent mean ± SEM of n = 4–5 mice/group. $^{*}P < .05$ between the indicated groups and vehicle-treated groups and $^{\#}P < .05$ between the JZL184-treated vs I/R vehicle-treated groups. EET, epoxyeicosatrienoic acid.

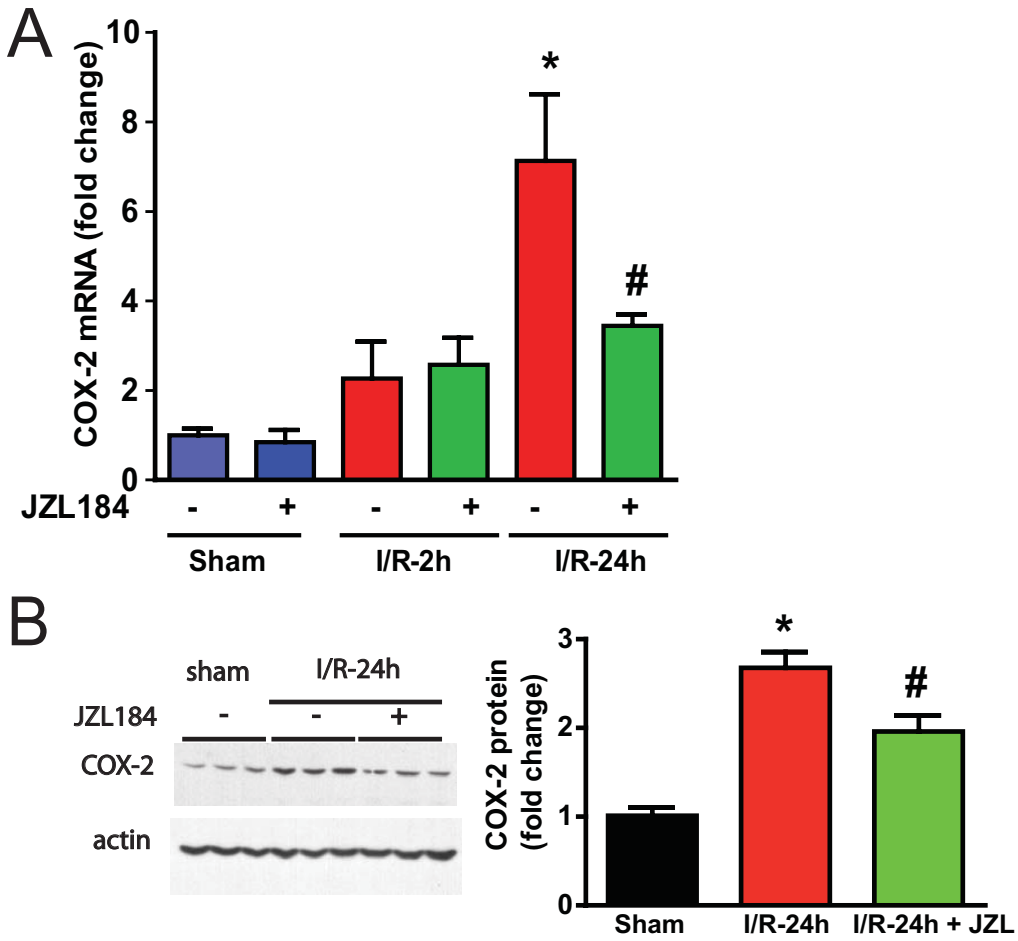

Supplementary Figure 2. MAGL inactivation attenuates hepatic COX-2 expression in the late phase of hepatic I/R. JZL184 pretreatment significantly suppressed elevations of hepatic COX-2 expression induced by 24 hours (but not 2 hours) of liver reperfusion (I/R-24h) as assessed by (*A*) real-time RT-PCR and (*B*) Western blotting. RT-PCR data represent mean ± SEM of n = 4–8 mice/group. $^{*}P < .05$ compared with the vehicle-treated sham groups and $^{\#}P < .05$ compared with the corresponding vehicle-treated I/R groups.

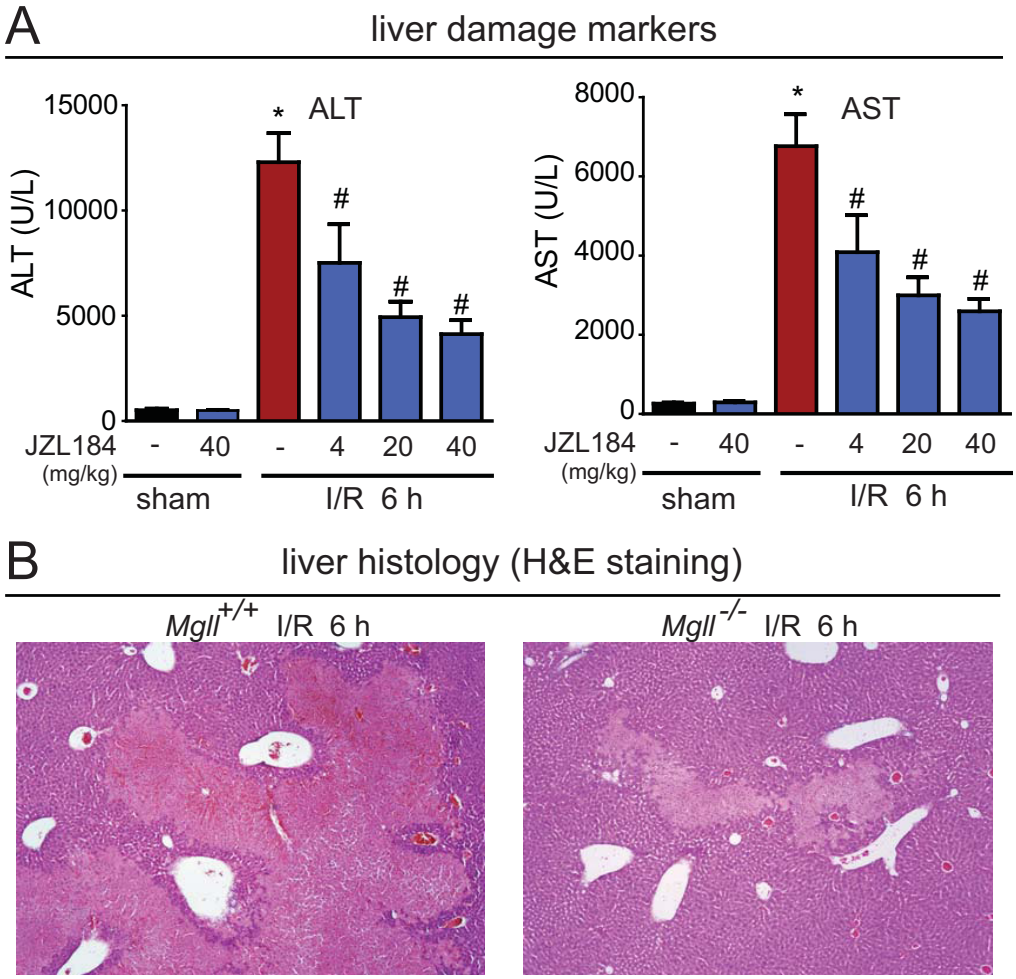

Supplementary Figure 3. MAGL inactivation attenuates hepatic I/R-induced tissue injury. (*A*) Liver damage/necrosis markers ALT and AST are significantly elevated in mouse serum upon I/R induction 6 hours after reperfusion and substantially reduced with pharmacologic blockade of MAGL (JZL184 IP) in a dose-responsive manner. (*B*) Liver histology (H&E staining) of mice subjected to 1 hour of ischemia followed by 6 hours of reperfusion (I/R 6 h) or sham surgery in $Mgll^{+/+}$ vs $Mgll^{-/-}$ mice, showing representative images of coagulation necrosis (*lighter areas*). Data represent mean ± SEM of n = 6–9 mice/group for *panel A*. $^{*}P < .05$ between vehicle-treated I/R groups vs sham vehicle-treated groups and $^{\#}P < .05$ between JZL184-treated I/R groups vs the corresponding I/R vehicle-treated groups.

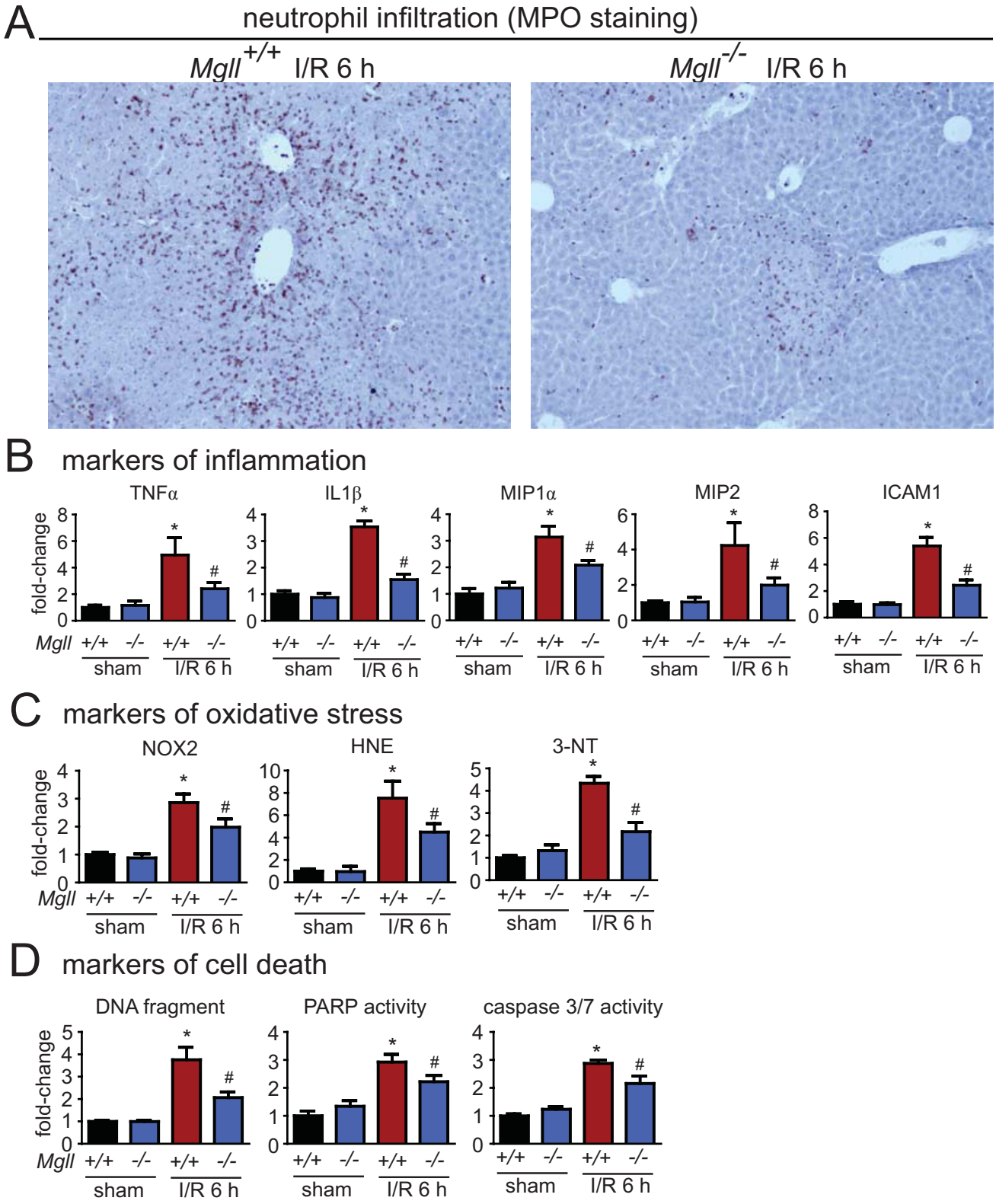

Supplementary Figure 4. MAGL inactivation attenuates hepatic I/R-induced inflammation and oxidative stress. (*A*) Genetic deletion of MAGL causes massive delayed infiltration of neutrophils as assessed by myeloperoxidase staining (*brown staining*) of livers after 6 hours of reperfusion following induction of 1 hour of hepatic ischemia (I/R 6 h). Representative images are shown. This neutrophil infiltration is significantly attenuated in $Mgll^{-/-}$ I/R mice. (*B–D*) The I/R-induced elevations in proinflammatory cytokines and chemokines TNF-α, IL-1β, MIP1-α, and MIP-2; adhesion molecule ICAM-1; oxidative stress markers NOX2, HNE, and 3-NT; and cell death markers DNA fragmentation, PARP activity, and caspase 3/7 activity assessed after 6 hours of reperfusion (I/R 6 h) are significantly attenuated in $Mgll^{-/-}$ mice. Data represent mean ± SEM of n = 6–12 mice/group. $^{*}P < .05$ compared with sham surgery of $Mgll^{+/+}$ groups and $^{\#}P < .05$ between $Mgll^{-/-}$ I/R groups and the corresponding $Mgll^{+/+}$ I/R groups.

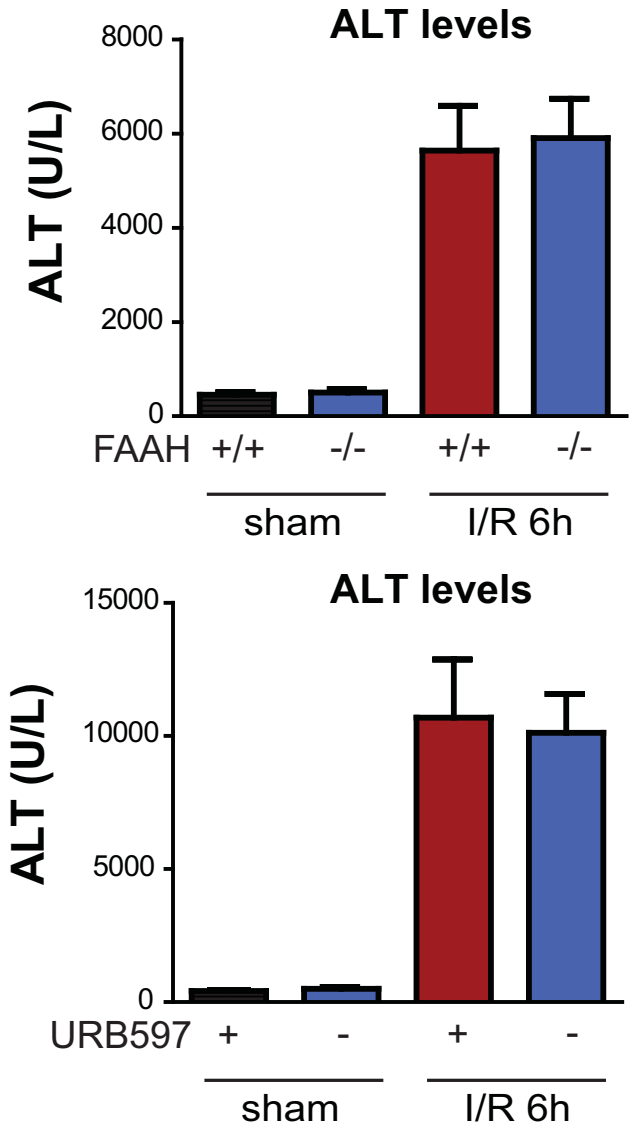

Supplementary Figure 5. FAAH inactivation does not protect against hepatic I/R-induced tissue injury. Liver damage/necrosis markers ALT are significantly elevated in mouse plasma on I/R induction 6 hours after reperfusion and are not reduced with pharmacologic blockade of FAAH (URB597, 10 mg/kg IP, *lower panel*) or in $FAAH^{-/-}$ mice (*upper panel*). Data represent mean ± SEM of n = 6 mice/group.

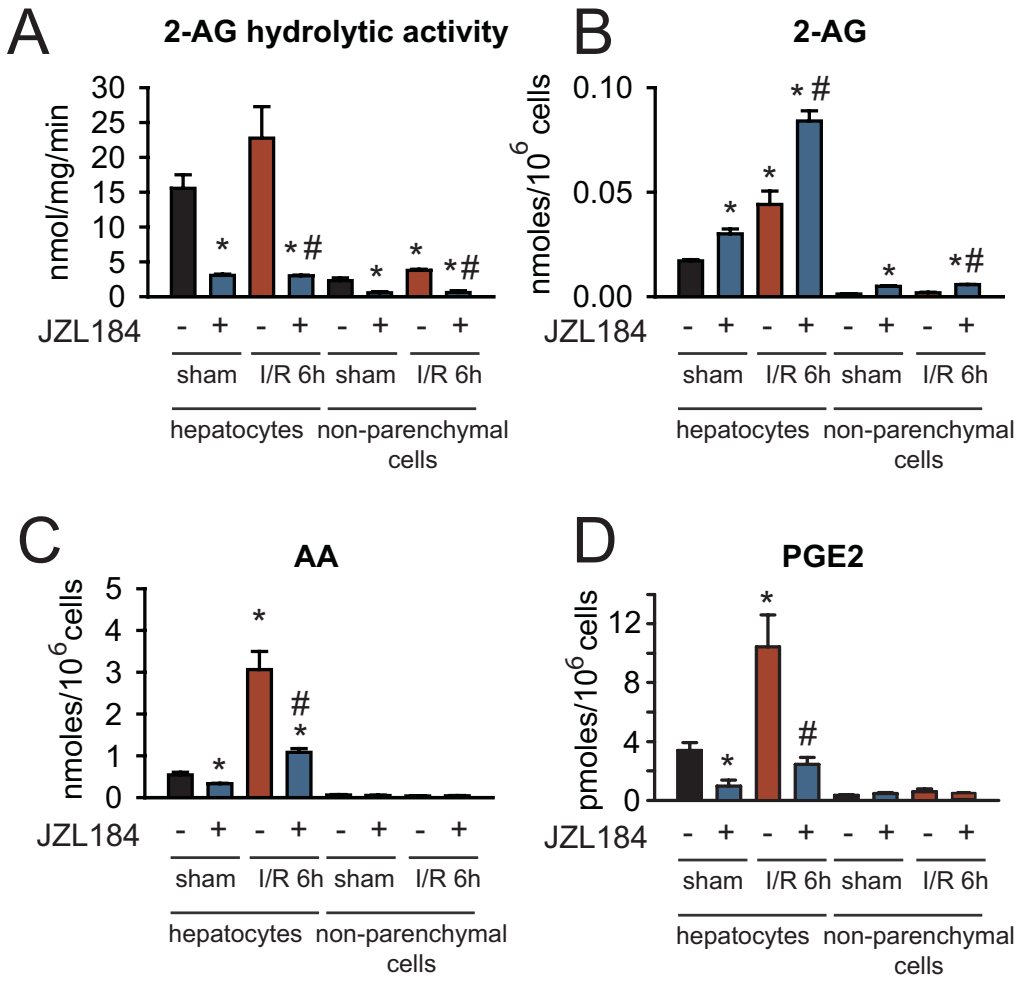

Supplementary Figure 6. Cell type–specific control of MAGL over endocannabinoid and eicosanoid metabolism. (*A*) MAGL activity is significantly higher in hepatocytes vs nonparenchymal cells as assessed by 2-AG hydrolytic MAGL activity monitoring the release of AA. Mice were treated in vivo with JZL184 (40 mg/kg IP) 1 hour before I/R for 6 hours and then livers were removed and hepatocytes and nonparenchymal cells were isolated. (*B–D*) 2-AG, AA, and PGE_2 levels are elevated in hepatocytes but not in nonparenchymal cells on I/R. MAGL blockade elevates 2-AG levels in hepatocytes and nonparenchymal cells, whereas it lowers AA and eicosanoid levels only in hepatocytes. Data represent mean ± SEM of n = 3–4 mice/group. $^{*}P < .05$ compared with vehicle-treated groups within hepatocytes or nonparenchymal cells and $^{\#}P < .05$ between JZL184-treated I/R groups and the corresponding vehicle-treated I/R groups.

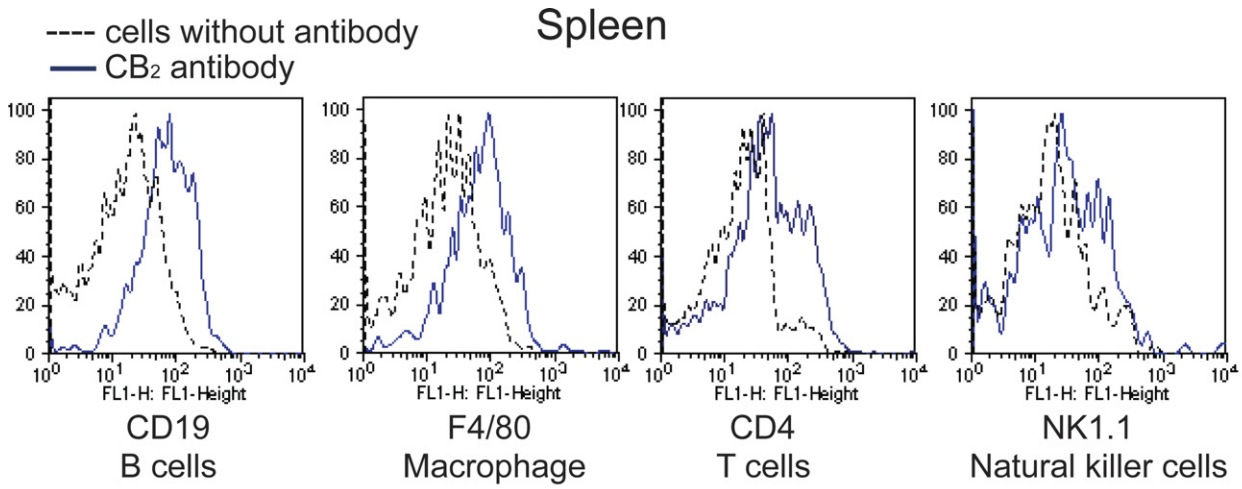
---- cells without antibody
— CB2 antibody
Spleen
FL1-H: FL1-Height
CD19
B cells
F4/80
Macrophage
CD4
T cells
NK1.1
Natural killer cells

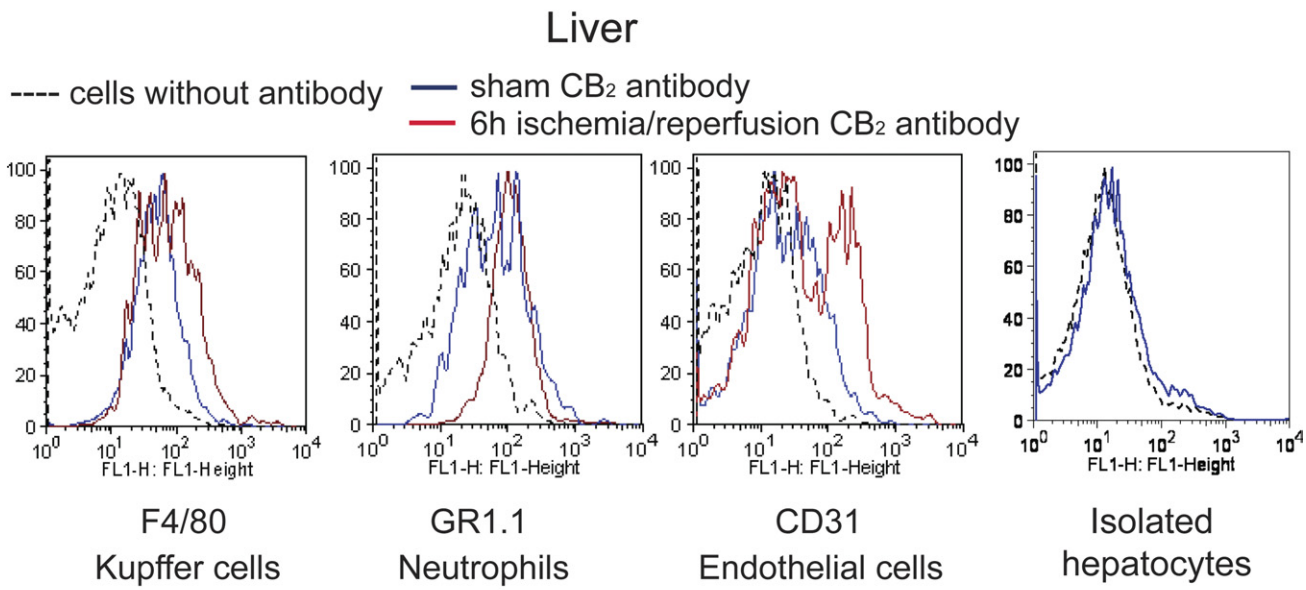
Liver
---- cells without antibody
— sham CB2 antibody
— 6h ischemia/reperfusion CB2 antibody
FL1-H: FL1-Height
F4/80
Kupffer cells
GR1.1
Neutrophils
CD31
Endothelial cells
Isolated
hepatocytes

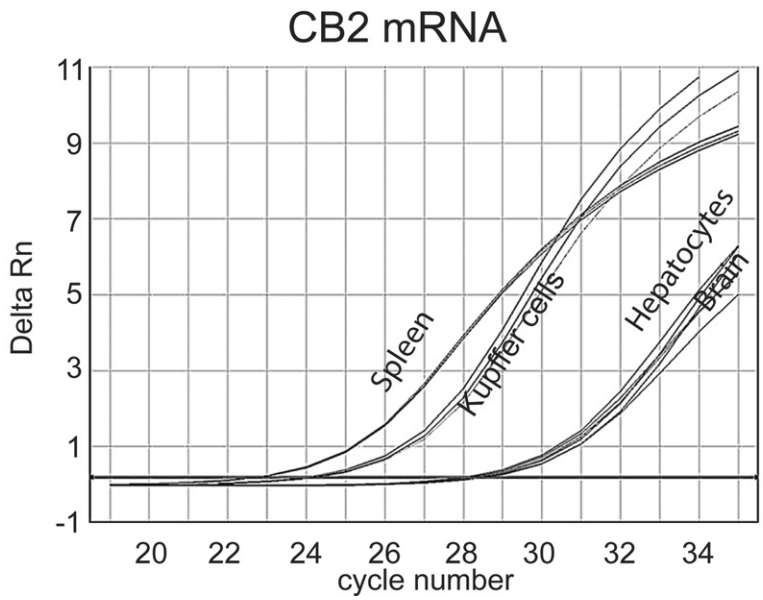
CB2 mRNA
Delta Rn
cycle number
Spleen
Kupffer cells
Hepatocytes
Brain

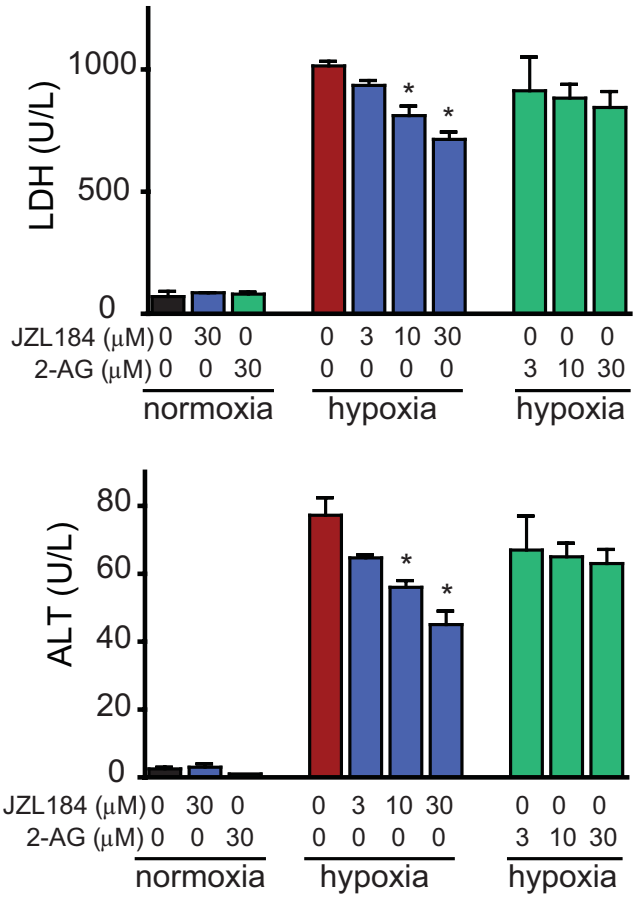

Supplementary Figure 8. MAGL blockade but not 2-AG protects hepatocytes against hypoxia/reoxygenation-induced cell death. Primary mouse hepatocytes were subjected to 12 hours of hypoxia, followed by 12 hours of reoxygenation. Pretreatment with JZL184, but not 2-AG, reduces hepatocyte cell death in a concentration-dependent manner, as determined by lactate dehydrogenase (*upper panel*) and ALT (*lower panel*) levels in the culture medium. Data are expressed as mean ± SEM (n = 2–4 replicates/group) of a representative experiment from 3 independent experiments. $^{*}P < .05$ vs vehicle-treated hypoxia group.

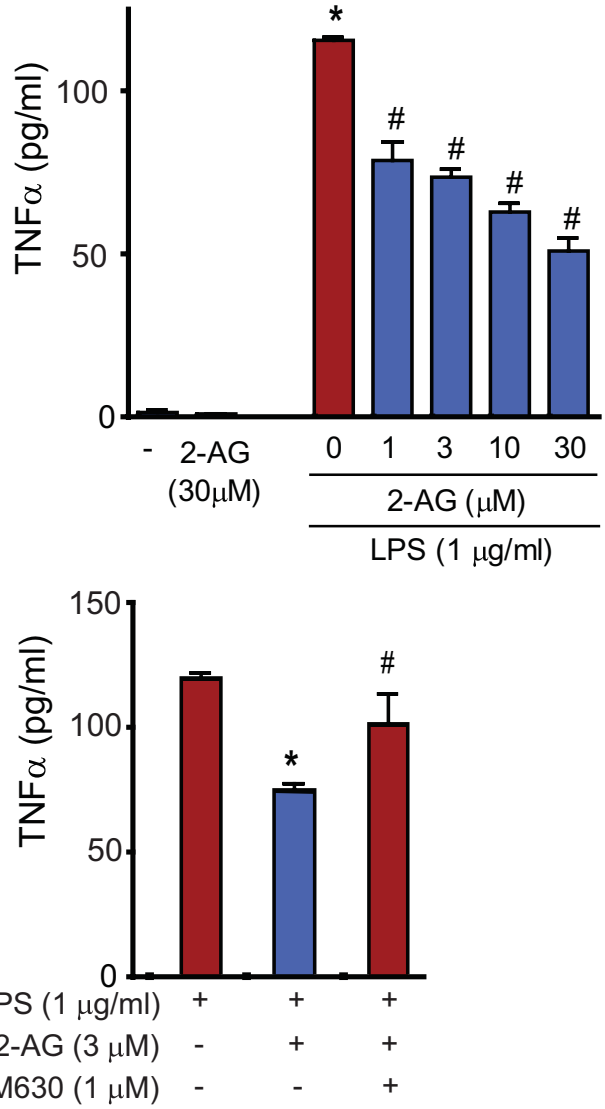

Supplementary Figure 9. 2-AG suppresses LPS-induced TNF-α release from KCs. 2-AG treatment of isolated KCs shows a concentration-dependent reduction in LPS-stimulated TNF-α release, determined by ELISA (*upper panel*). This reduction is partially attenuated by treatment with the CB_2 antagonist AM630, but only at lower concentrations of 2-AG (*lower panel*). Data represent mean ± SEM of n = 3–4 replicates/group. Each experiment was performed at least 3 times independently. $^{*}P < .05$ vs vehicle-treated control groups; $^{\#}P < .05$ vs LPS only treated group (*upper panel*) or $^{*}P < .05$ vs LPS only treated groups; $^{\#}P < .05$ vs LPS + 2AG–treated group (*lower panel*).

←

Supplementary Figure 7. Cell type specificity of CB_2 expression. *Upper panels* show representative histogram plots of CB_2 surface expression in splenic B cells ($CD19^+$ cells), macrophages ($F4/80^+$ cells), T cells ($CD4^+$ cells), and natural killer cells ($NK1.1^+$ cells). *Histogram with dashed line* represents background without any CB_2 antibody, whereas *histogram with blue line* represents CB_2 expression. *Middle panels* show representative histogram plot of CB_2 surface expression in liver KCs ($F4/80^+$ cells), neutrophils ($Gr1.1^+$ cells), endothelial cells ($CD31^+$ cells), and hepatocytes. *Histogram with dashed line* represents background without any CB_2 antibody, *histogram with blue line* represents CB_2 expression in sham control mice, and *red lines* are from I/R 6h samples. *Lower panel* shows CB_2 mRNA expression detected by real-time PCR amplification for various cell types/tissues as indicated. Spleen serves as positive and brain as negative control for CB_2 expression.

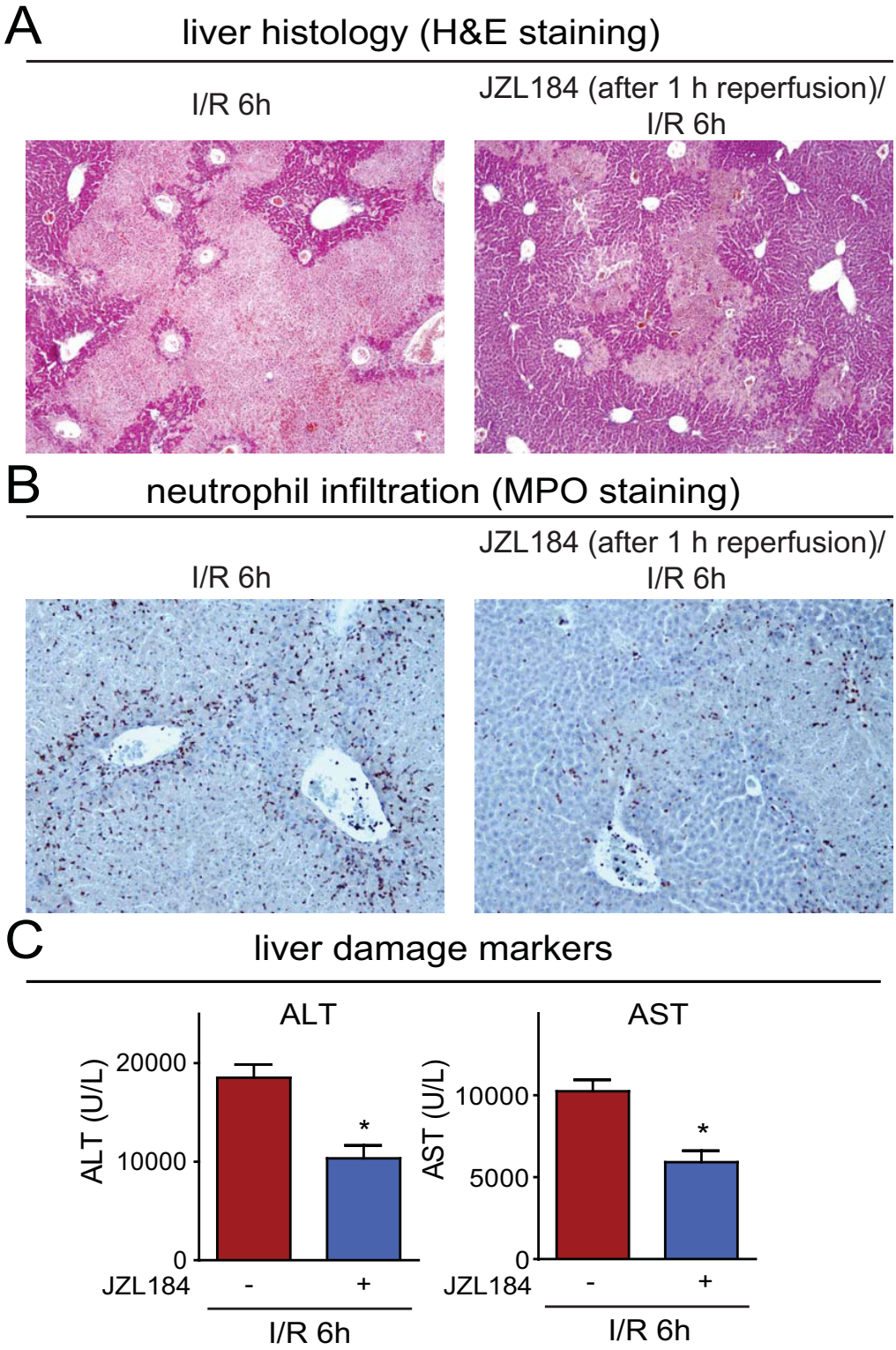

Supplementary Figure 10. MAGL inhibition exerts hepatoprotection even when given after reperfusion. (*A*) Coagulation necrosis, (*B*) neutrophil infiltration, and (*C*) liver damage markers ALT and AST are reduced in hepatic I/R even when JZL184 is administered at 1 hour of reperfusion. All parameters were measured at 6 hours of reperfusion (6h I/R). Data represent mean ± SEM with n = 6 mice/group. $^{*}P < .05$ between the JZL184 I/R group and the vehicle-treated I/R group.

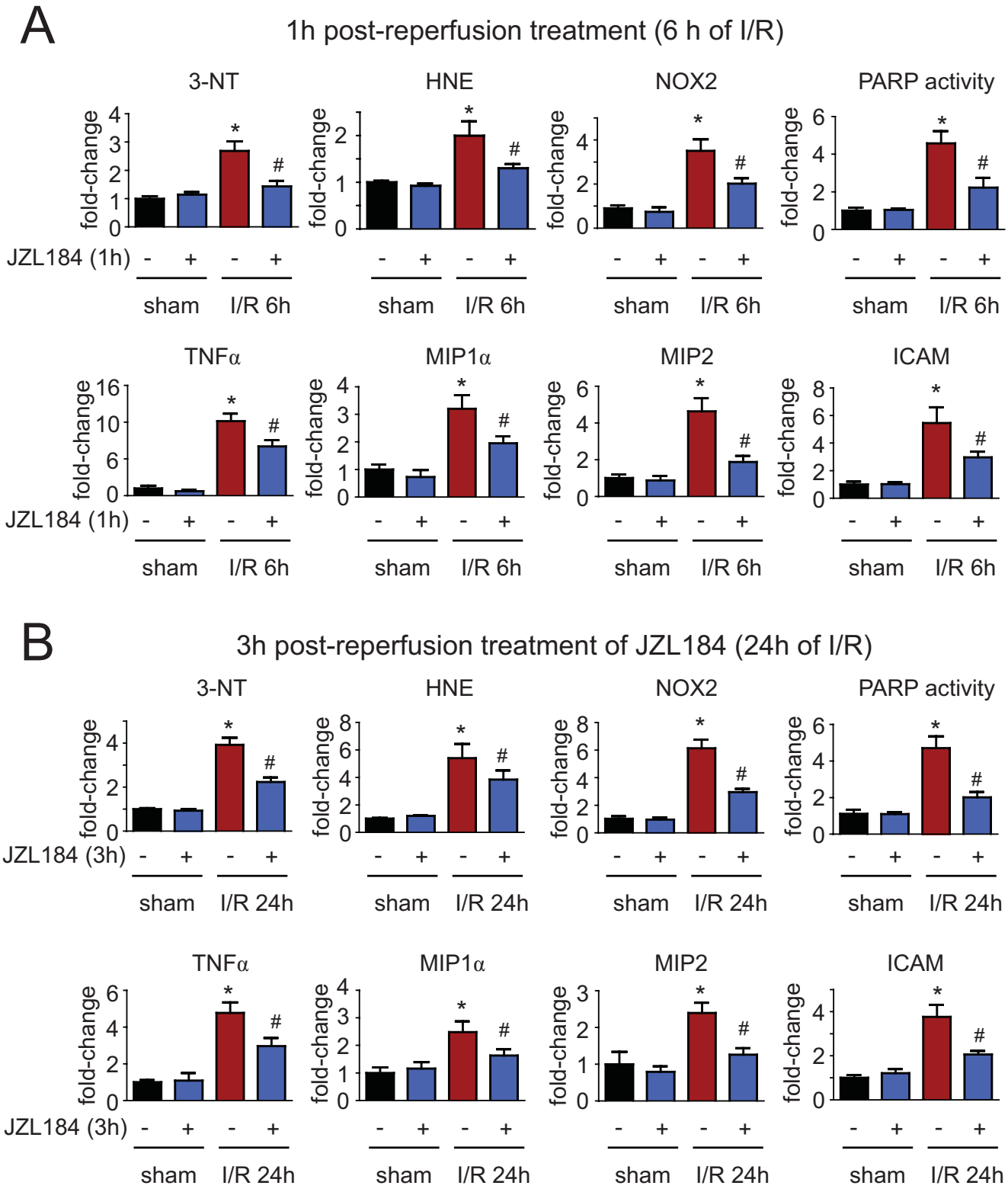

Supplementary Figure 11. MAGL inactivation attenuates hepatic I/R-induced inflammation and oxidative stress, even when MAGL inhibitors are given after reperfusion. The I/R-induced elevations in proinflammatory cytokines and chemokines, adhesion molecule ICAM-1, oxidative stress markers, and cell death markers assessed after (*A*) 6 or (*B*) 24 hours of reperfusion (I/R 6 h, I/R 24 h) are significantly attenuated in JZL184-treated mice (1 or 3 hours after reperfusion). Data represent mean ± SEM of n = 6–12 mice/group. $^{*}P < .05$ between the indicated groups and sham surgery vehicle-treated groups and $^{\#}P < .05$ between JZL184-treated I/R groups and the corresponding vehicle I/R groups.

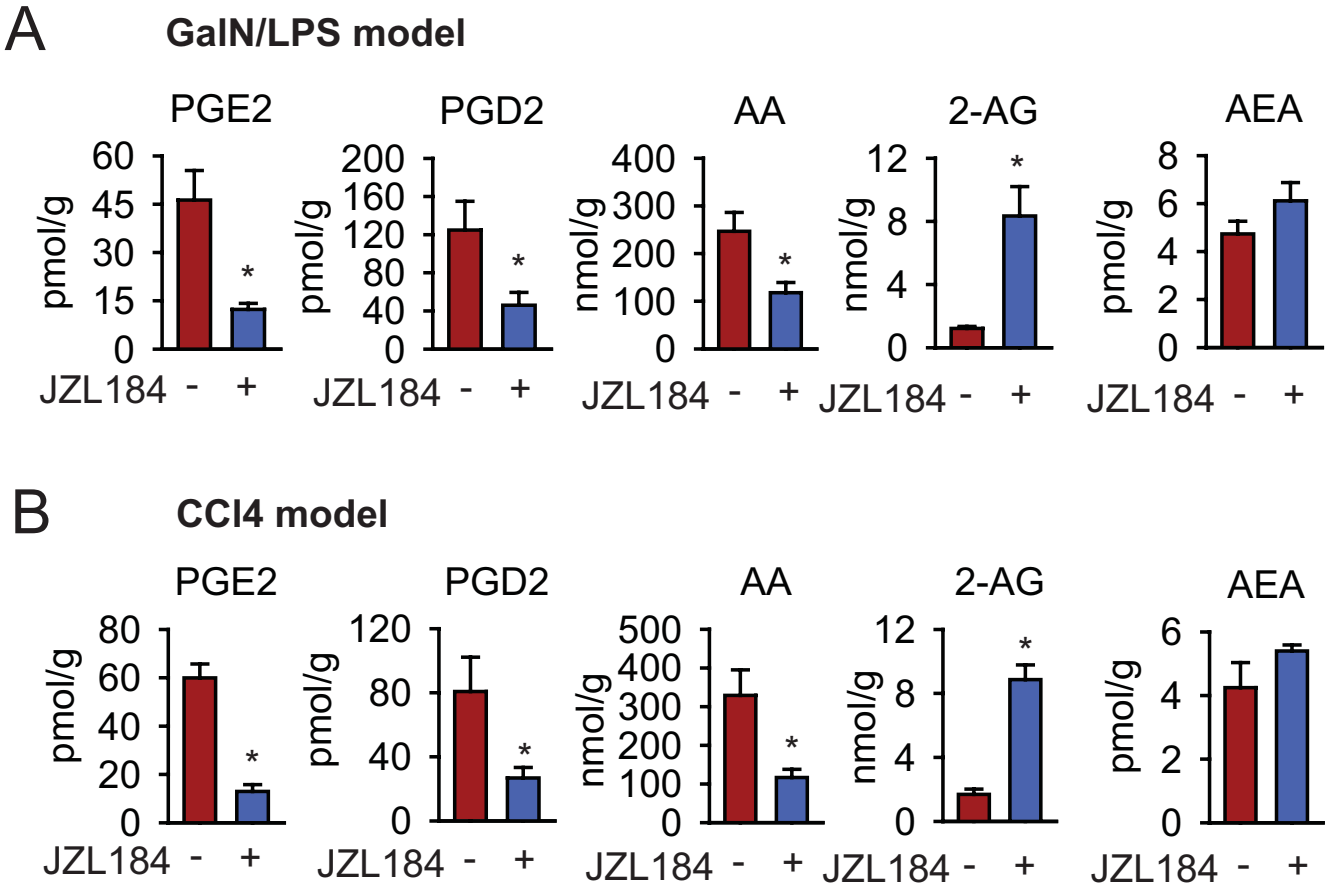

Supplementary Figure 12. MAGL inactivation exerts bidirectional control over endocannabinoid and eicosanoid levels in GalN/LPS or CCl_4-induced acute liver injury models. (*A* and *B*) Inactivation of MAGL by JZL184 enhances 2-AG levels but does not affect the levels of the other endocannabinoid anandamide in livers of GalN/LPS or CCl_4-treated mice. MAGL blockade lowers AA and eicosanoids in livers of GalN/LPS or CCl_4-treated mice. Data represent mean ± SEM of n = 5–8 mice/group. $^*P < .05$ between GalN/LPS or CCl_4-treated groups and the control groups without JZL184.

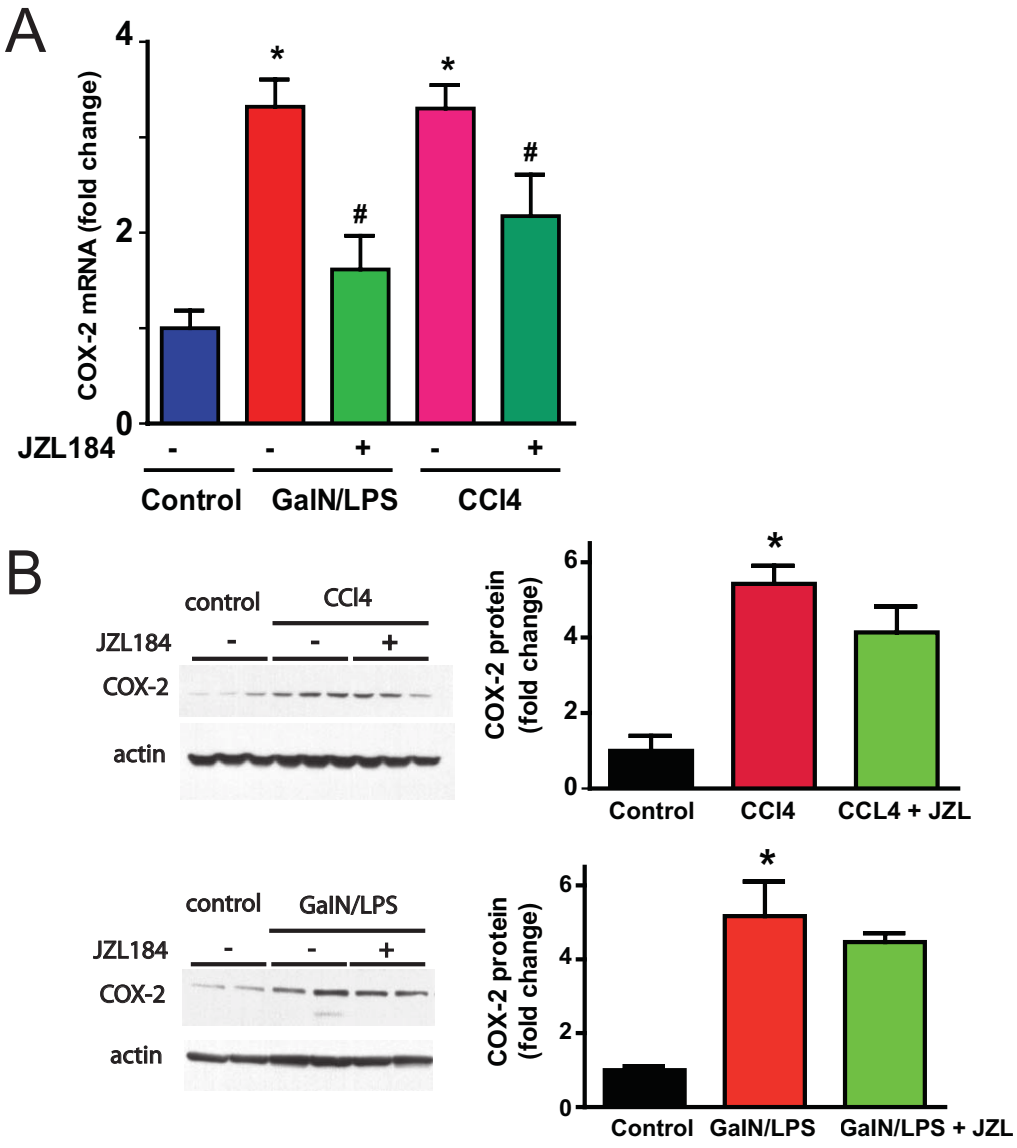

Supplementary Figure 13. MAGL inactivation attenuates hepatic COX-2 mRNA but not protein levels in GalN/LPS or CCl_4-induced liver injury models. JZL184 pretreatment significantly suppressed elevations of (*A*) hepatic COX-2 mRNA but not (*B*) protein expression induced by GalN/LPS or CCl_4 treatments, as assessed by real-time reverse-transcription PCR or Western blotting. Data represent mean ± SEM of n = 4–8 mice/group. $^{*}P < .05$ compared with the vehicle-treated control groups and $^{\#}P < .05$ compared with the corresponding vehicle-treated GalN/LPS or CCl_4 groups.